Journal of Structural Geology 167 (2023) 104781

Contents lists available at ScienceDirect

Journal of Structural Geology

journal homepage: www.elsevier.com/locate/jsg

West Spitsbergen fold and thrust belt: A digital educational data package for teaching structural geology

Rafael Kenji Horota [a,b,*], Kim Senger [a], Nil Rodes [a], Peter Betlem [a,c], Aleksandra Smyrak-Sikora [a], Marius O. Jonassen [d], Daniel Kramer [e], Alvar Braathen [c]

[a] Department of Arctic Geology, The University Centre in Svalbard, PO Box 156, 9171, Longyearbyen, Norway
[b] Department of Earth Science, University of Bergen, Allégaten 41, 5020, Bergen, Norway
[c] Department of Geosciences, University of Oslo, Sem Sælands Vei 1, 0371, Oslo, Norway
[d] Department of Arctic Geophysics, The University Centre in Svalbard, PO Box 156, 9171, Longyearbyen, Norway
[e] Department of Applied Geosciences, University of Sherbrooke, 2500, Boul. de L'Université, Sherbrooke (Québec) J1K 2R1, Canada

ARTICLE INFO

Keywords:
Svalbard
Compressional
Digital
Education
Faulting

ABSTRACT

The discipline of structural geology is taking an advantage of compiling observations from multiple field sites to comprehend the bigger picture and constrain the region's geological evolution. In this study we demonstrate how integration of a range of geospatial digital data sets that relate to the Paleogene fault and thrust belt exposed in the high Arctic Archipelago of Svalbard, is used in teaching in bachelor-level courses at the University Centre in Svalbard. This event led to the formation of the West Spitsbergen Fold and Thrust Belt and its associated foreland basin, the Central Spitsbergen Basin. Our digital educational data package builds on published literature from the past four decades augmented with recently acquired high-resolution digital outcrop models, and 360° imagery. All data are available as georeferenced data containers and included in a single geodatabase, freely available for educators and geoscientists around the world to complement their research and fieldwork with course components from Svalbard.

1. Introduction

The ability to envision and connect geological features across time and space is a fundamental principal to the geosciences and one of the key learning objectives that must be addressed in the education of geoscientists (Kastens et al., 2009). Outcrops, defined as semi-three-dimensional spatial elements, play an important role in demonstrating geological principles (Kastens and Ishikawa, 2006). Along with other multi-scale representations of geological structures, such as geological maps and cross-sections, geoscientists determine and reconstruct geological processes in the context of regional structural history. In other words, after acquiring the data, a geoscientist must integrate multi-scale data, from outcrop to satellite imagery, to propose a conceptual geological evolution of the studied region (e.g., Hodgetts, 2013).

Traditionally, outcrop data collection and changes in visual perspectives depended on the geoscientists' physical ability to access the outcrop and conduct structural (e.g., scanlines, orientation and kinematic indicators of faults) and sedimentological (e.g., sedimentary logs, sampling) studies. Depending on the outcrop conditions, such as exposure, steepness, and accessibility, much of the studied outcrop may be sub-sampled with observations possible at selected places. These physical restrictions are more evident in isolated and remote places like the Arctic archipelago of Svalbard, where the summer field season extends from June to September and glacier ice covers about 60% of the land (Senger et al., 2021c). Fieldwork for data collection purposes in this environment is excellent given that its pristine outcrops are well suited for analogue studies, data collection and field-teaching. Physical restrictions on access can be overcome with longer field campaigns with increased funding. However, fieldwork is also an integral component of geosciences education courses where funding is limited, and despite the associated positive social and learning outcomes, it has been targeted for cuts in many universities worldwide (Dolphin et al., 2019). This is mainly because field trip offerings include the cost of liability insurance and increasing budgets are necessary to support staff salaries (Baker, 2006; Boyle et al., 2007). In these activities, the physically challenging nature of geological fieldwork also plays a significant role in limiting access, especially for students with mobility and sensory disabilities

* Corresponding author. Department of Arctic Geology, The University Centre in Svalbard, PO Box 156, 9171, Longyearbyen, Norway.
E-mail address: rafaelh@unis.no (R.K. Horota).

https://doi.org/10.1016/j.jsg.2022.104781
Received 31 March 2022; Received in revised form 6 December 2022; Accepted 30 December 2022
Available online 6 January 2023

(Atchison and Feig, 2011; Atchison and Libarkin, 2013; Gilley et al., 2015). Furthermore, the Covid-19 pandemic highlighted the increasing need of integrating digital field access.

Throughout the past decade, the geosciences have undergone a major revolution driven by technological advancements in the collection and capacity of processing remote sensing data. Structure-from-motion photogrammetry from consumer drones is particularly effective in cost-effectively generating high-quality geo-referenced digital outcrop models (DOMs; Bemis et al., 2014; Chesley et al., 2017; Vollgger and Cruden, 2016; Westoby et al., 2012). Compared to standard field photographs, DOMs allow quantitative measurements of geological features and a change in perspective. This is especially useful when appreciating structural features such as folds and faults from different vintage points. In parallel, the decreasing cost and size of Lidar scanners have allowed the acquisition of digital models across scales and devices, including smartphones (Luetzenburg et al., 2021; Tavani et al., 2022), mobile sensor units (Goelles et al., 2022) and the more traditionally used tripod-based terrestrial Lidar scanners (Buckley et al., 2008). By facilitating access to outcrop field observations, DOMs allow geoscientists to digitally integrate observations over a range of scales and bridge the gap between the wellbore and seismic scales (e.g., Marques et al., 2020; Rarity et al., 2014). Digital outcrop databases like e-Rock (Cawood and Bond, 2019), V3Geo (Buckley et al., 2022), digital Australia and MOSIS (Gonzaga et al., 2018) provide excellent multi-scale and multi-resolution DOMs as well as complementary data such as 360° imagery. However, these data sets often lack the context of the "bigger" picture, such as the overall tectonic regime. Complementary data sets, ranging from basin-scale (e.g., gravity, magnetic, geological, and paleogeographic maps) to subsurface data (e.g., borehole, seismic, electromagnetic) to outcrop-scale (e.g., sedimentological and structural observations, samples), can provide this context if these are properly spatially integrated with the DOMs. We try to provide such a seamless integration through the Svalbox database (Betlem et al., in review; Senger et al., 2021a, 2021c). Svalbox is a web- and Petrel-based portal that offers open access to Svalbard's geoscientific data, including DOMs, 360° imagery, and subsurface data. This approach mimics that of a professional geologist, who often needs to place fragmented information from a range of sources together to comprehend the bigger picture. Data

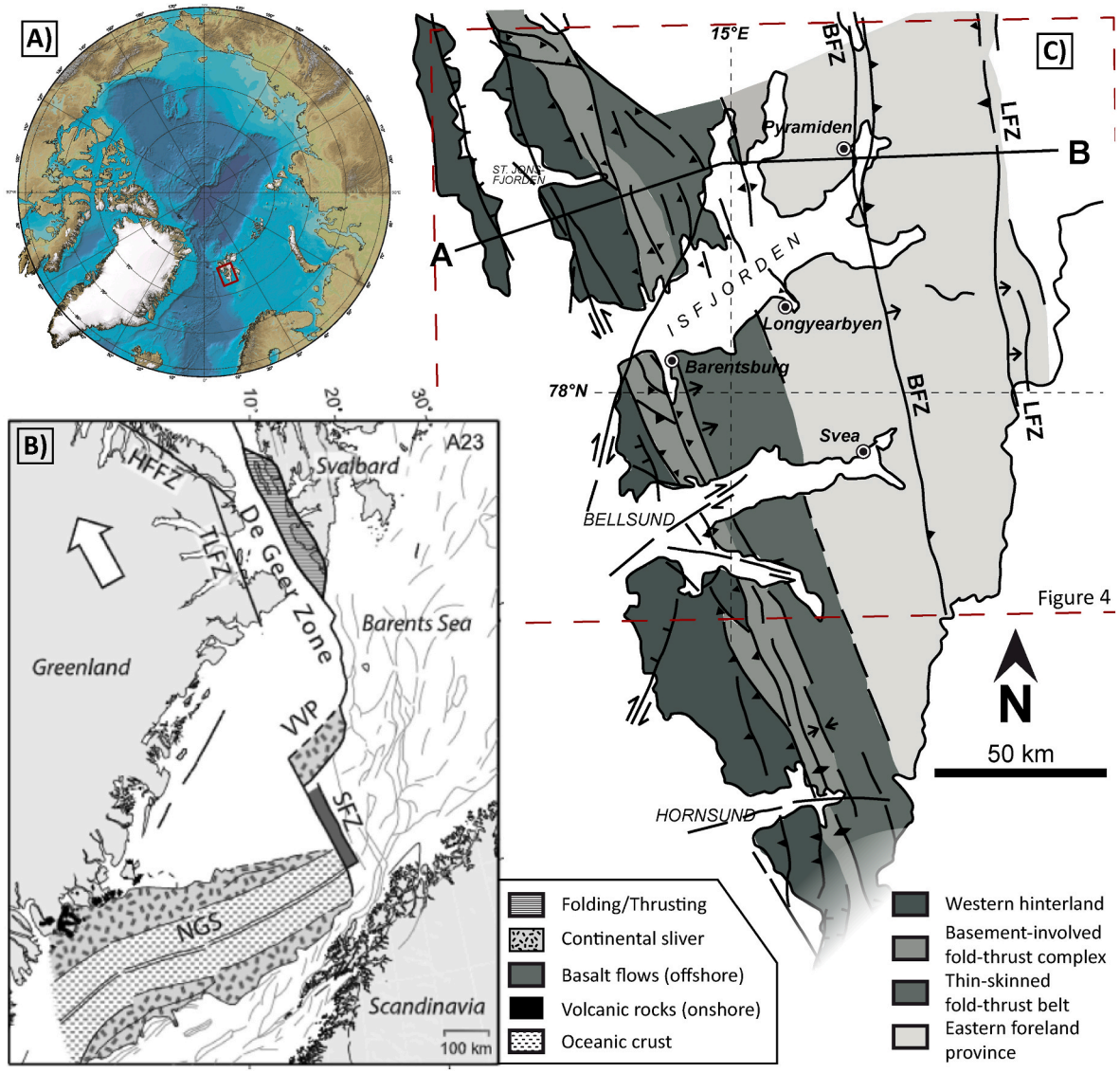

Fig. 1. A) Location of the Svalbard archipelago. B) Regional geodynamic setting of Svalbard in the north Atlantic. VVP = Vestbakken Volcanic Province, SFZ = Senja Fracture Zone, NGS = Norwegian-Greenland Sea, HFFZ = Harder Fjord Fault Zone, TLFZ = Trolle Land Fault Zone. Map from Leever et al. (2011). C) Tectonic map of the study area (from Ogata et al., 2014; originally published by Bergh et al. (1997)), illustrating the overall structural setting of the profile presented in profile AB (Fig. 3).

integration across scales, and with different data types, is crucial to understand basin evolution, and is perhaps best exemplified through the integrative work conducted in the petroleum industry (Howell et al., 2014; Marques et al., 2020; Pringle et al., 2006). However, the challenge is that relevant data are rarely compiled and made accessible to conduct basin-scale training/research projects.

In this contribution, we provide a digital educational data package that details the structural evolution of Spitsbergen along a ca. 200 km long E-W cross-section, integrating a wide range of geoscientific data from the Svalbox database that are openly available to the global geoscience community. The cross-section crosses the West Spitsbergen Fold and Thrust Belt (WSFTB) and its associated foreland basin, as well as long-lived N–S trending structural lineaments. All data types are geospatially linked as georeferenced data containers that are pre-loaded in ArcGIS Pro, QGIS, and Petrel projects. Individual elements are also included in digital formats (GeoTiffs, shapefiles, pdf) to facilitate inclusion in other software packages. Furthermore, we discuss the potential of such digital educational packages in overcoming one of the main challenges in geoscience education, spatial thinking. Spatial thinking involves appreciation of scales, orientations of 3D (and 4D due

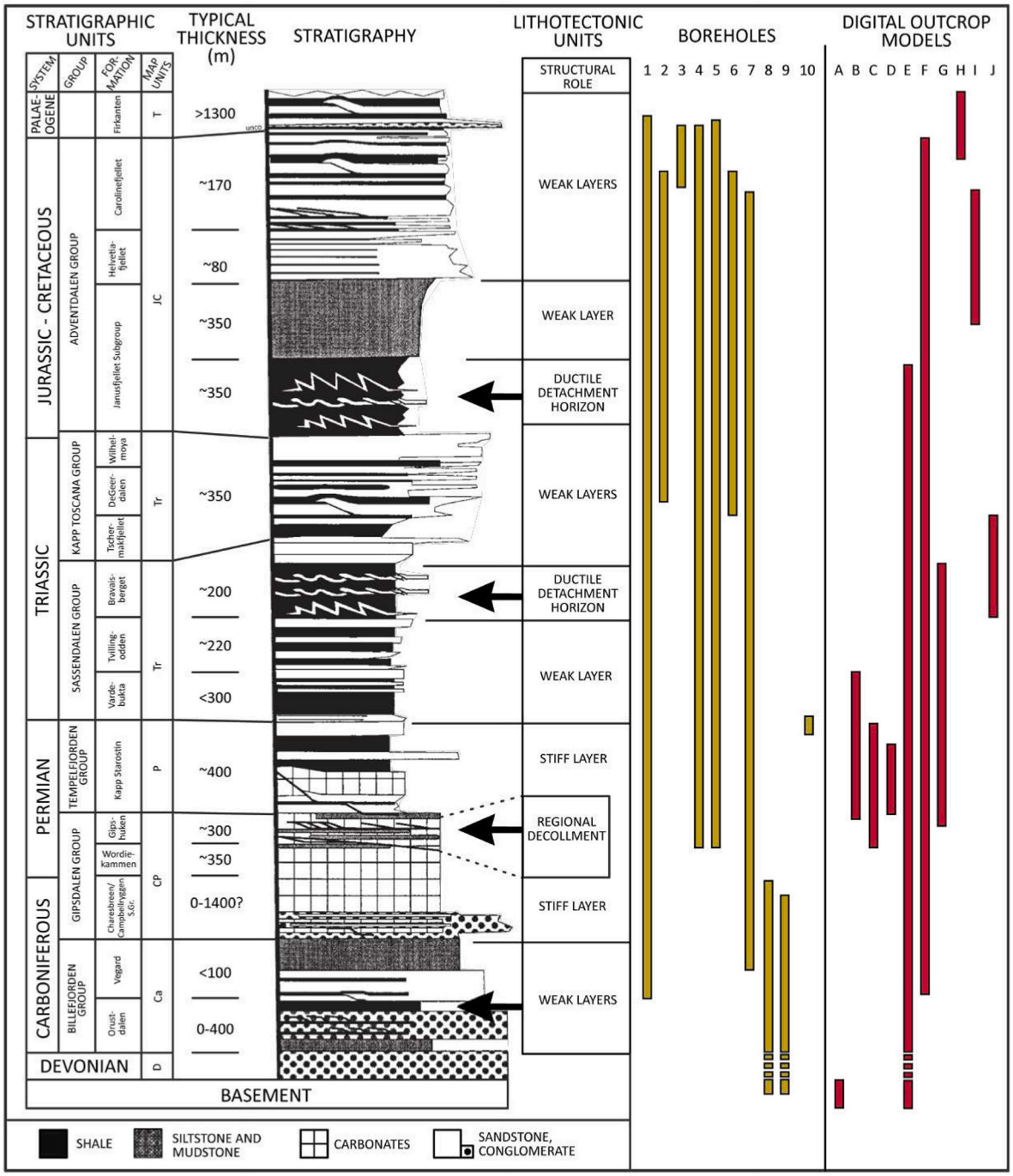

Fig. 2. Regional stratigraphic column of the study area from Braathen and Bergh (1995), illustrating the overall lithologies, cumulative stratigraphic thickness and regional decollement layers in mechanically weak units. The legend indicates the approximate stratigraphic position of a selection of boreholes and DOMs. Borehole data abbreviations: 1 - Vassdalen II; 2 - Grønnfjorden I; 3 - Kapp Laila I; 4 - Colesbukta; 5 - Ishøgda I; 6 - DH4; 7 - Reindalspasset I; 8 - Petuniabukta coal; 9 - Gipsdalen coal; 10 - Deltadalen P-T. DOMs abbreviations: A - Lagmannstoppen; B - Akseløya; C - Värmlandryggen; D - Productustoppen; E – Midterhuken; F - Festningen; G - Mediumfjellet; H - Firkanten; I - Janusfjellet; J - Eistradalen, Table 2. Figure modified from Braathen et al. (1999).

to the time effect) features and interlinkage of observations from multiple field sites.

2. Geological setting

Svalbard is located on the north-western corner of the Eurasian plate (Fig. 1A and B). The bedrock geology of Svalbard rocks can be traced offshore to the south and east and thus provide insights into both the petroleum-bearing provinces of the south-western Barents Sea (Henriksen et al., 2011) and the circum-Arctic basins (Grantz et al., 2011). Svalbard is bounded by a sheared margin to the west, a steep passive margin to the north, and transitions into the submerged part of the Barents Shelf to the south and east (Fig. 1B). The geological evolution of Svalbard is well covered in synthesis contributions, for instance by Steel and Worsley (1984), Worsley (2008), Dallmann (2015) and Olaussen et al. (2023) and is only briefly outlined here, focussing on the major tectonic events and the involved lithologies.

We frame the geological setting around a tectonic map (Fig. 1), a regional stratigraphic column (Fig. 2), and an east-west cross-section across Svalbard (Fig. 3). Geological and topographic maps are provided online (Norwegian Polar Institute, 2016, 2022a) and streamed directly to the Svalbox online portal. The Svalbard archipelago comprises all islands between 74 and 81°N and 15–35°E, including the main islands of Spitsbergen, Nordaustlandet, Barentsøya, Edgeøya, Prins Karls Forland, Hopen, and Bjørnøya (Fig. 1). Svalbard's Devonian-Paleogene sedimentary succession is nearly complete and comprises a wide range of lithologies (conglomerates, sandstones, shales, carbonates, evaporites) reflecting both Svalbard's general northward drift over geological time and local-regional tectonic influences (Fig. 2). Localized Quaternary volcanism and significant seismicity testify to Svalbard's dynamic nature (Minakov, 2018). Significant pre-glacial and Quaternary glaciations-deglaciations related uplift, led to Svalbard's emergence along with the rest of the Barents Shelf (Lasabuda et al., 2021).

Major tectonic events impacting the bedrock of Svalbard include the Caledonian orogeny, which occurred in response to the collision of Laurentia and Baltica (Harland and Horsfield, 1974). Pre-Devonian metamorphic and sedimentary basement rocks that were involved in the Caledonian orogeny are exposed in northern Svalbard and along the western coast, while in central Spitsbergen they underlie the younger strata (Fig. 3). Late or post-Caledonian Orogeny, orogenic collapse has been inferred from extensional detachments underneath Devonian Old Red Sandstone deposits (Braathen et al., 2018; Maher et al., 2022). The Late Devonian post-Caledonian Ellesmerian-Svalbardian compressional event caused west-verging folding and faulting, mainly along the eastern flank of the Devonian basin in NW Spitsbergen (Piepjohn, 2000), although some of these folds appear related to the extensional collapse as major, transport-parallel corrugations (Maher et al., 2022). The Devonian succession crops out in north-central Spitsbergen and in the south, in Hornsund, and is overlain unconformably by Permo-Carboniferous successions, which are topped by Mesozoic units (Figs. 2 and 3). Mid-to Late Carboniferous rifting localized along pre-existing N–S lineaments led to the development of narrow sedimentary basins, including the well-known Billefjorden Trough that developed along the eastern flank of the Billefjorden Fault Zone (BFZ; Fig. 1C; Smyrak-Sikora et al., 2021). The BFZ and the Lomfjorden Fault Zone (LFZ) in the east, and St Jonsfjorden trough within the WSFTB (Braathen et al., 1995; Welbon and Maher, 1992) are schematically shown along the east-west cross-section (Fig. 3). Post-rift Permian carbonate platforms developed across a broad, epicontinental shelf sea that flooded the structural highs and covered most of Spitsbergen. Svalbard's northward drift was most rapid during the Permian (Dallmann, 2015), contributing to a shift from warm-water carbonates interbedded with evaporites to cold-water carbonate formation (Sorento et al., 2020; Stemmerik and Worsley, 2005). The Mesozoic was dominated by siliciclastic, mainly deep to shallow marine deposition and termination of carbonate factories. Small deltas were shedding sediments in early Triassic accommodation, first from a westerly source in Greenland before shifting to a regional south-easterly source in the Late Triassic from the Uralian orogeny (Anell et al., 2014; Glørstad-Clark et al., 2011; Klausen et al., 2019; Lundschien et al., 2014). The middle Triassic organic-rich shales deposited in front of the world's largest delta system are important regional source rocks (Wesenlund et al., 2021); however, on Svalbard these rocks also act as a major regional decollement zone for Paleogene transpression (Fig. 2; 3). Jurassic successions consist of

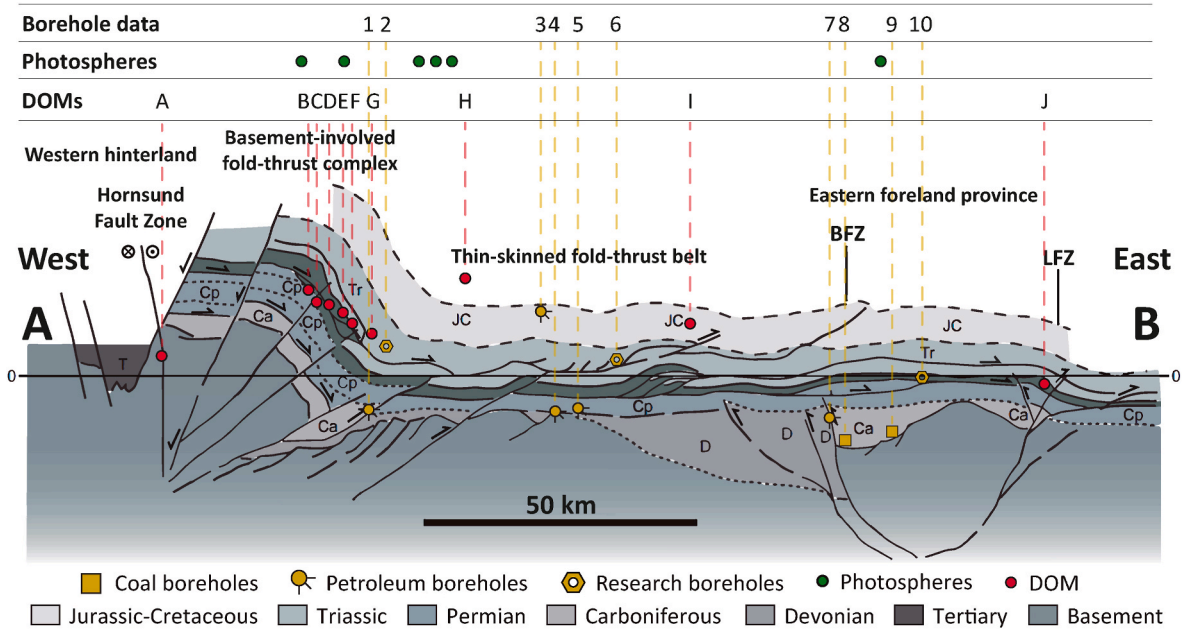

Fig. 3. East-west concept cross-section across the WSFTB, without the deposits of Central Spitsbergen Basin, highlighting the spatial variability of the major tectonic zones and datasets presented in this article. Refer to Fig. 1C for location of the cross-section. Elements (boreholes, DOMs, 360° imagery) not directly on the cross-section are projected onto it, see Fig. 4 for their true location. Figure modified from Ogata et al. (2014), originally published by Bergh et al. (1997). Abbreviations: BFZ – Billefjorden Fault Zone; LFZ – Lomfjorden Fault Zone; D – Devonian; Ca – Carboniferous; Cp – Permian; Tr – Triassic; JC – Jurassic–Cretaceous; T - Tertiary.

sandstones and conglomerates and represent the time-equivalent of important reservoirs for hydrocarbons on the Barents Shelf. They were also targeted for CO_2 sequestration in Svalbard (Mulrooney et al., 2019; Olaussen et al., 2019). The Jurassic reservoir rocks are capped by a thick succession of Late Jurassic-Early Cretaceous marine mudstones (Koevoets et al., 2018), that also act as a regional decollement zone (Fig. 2; Braathen et al., 1999). The following Cretaceous siliciclastic succession formed in response to a major regressive-transgressive cycle (Grundvåg et al., 2017; Midtkandal et al., 2019; Midtkandal and Nystuen, 2009). The northward sediment source is a consequence of uplift and tilt of Svalbard to the south that links to the development of major circum-Arctic magmatism associated with the High Arctic Large Igneous Province (HALIP). In Svalbard, HALIP is manifested as dykes, sills and lava flows of the Diabasodden Suite (Senger and Galland, 2022; Senger et al., 2014b). The longest hiatus in the Devonian-Paleogene sedimentary succession covers the entire Late Cretaceous, presumably related to HALIP activity.

In the Palaeogene, the Eurekan transpressional deformation, related to the opening and spreading in North Atlantic and Arctic Ocean, formed the WSFTB and the associated foreland basin, The Central Spitsbergen Basin (Helland-Hansen and Grundvåg, 2020). Thick-skinned tectonics involving metamorphic basement rocks dominate in western Spitsbergen (Bergh and Andresen, 1990; Bergh et al., 1997; Braathen et al., 1995, 1999), while the tectonic style in central Spitsbergen is thin skinned and east-vergent. Contractional strain by folding and thrusting are well developed in Mesozoic units, recording ENE-directed tectonic transport mainly above three regional detachments. The WSFTB forms a tectonic wedge, reflected in a foreland breaking thrust sequence. Thrust ramps place deformation higher in the Mesozoic stratigraphy to the east, whereas several out-of-sequence thrusts disrupt the overall progression. As commonly observed in fold-thrust belts, long thrust-flats, or detachments/decollements, and short thrust-ramps strongly influenced the geometry of the WSFTB. Detachments are localized within mechanically weak strata, namely Permian evaporites in the west, Middle Triassic mudstones in central parts, overlapping with and partly replaced by Late Jurassic mudstones farther east (Figs. 2 and 3). Paleogene transpression also re-activated some of the N–S lineaments including the BFZ, leading to inversion of Mid-Carboniferous rift-basins. These inversion monoclines interacted with thrust tectonics, seen as early thrusts folded in the monocline. Later thrusting decapitates and displaces the monocline eastward. The total amount of east-west crustal shortening during Paleogene transpression is estimated at 20–40 km (Bergh et al., 1997).

3. Methods and data

Here we highlight the data sets used (Table 1) and their contribution to understanding the tectonic evolution across the entire WSFTB. Key georeferenced data containers are identified in the stratigraphic column (Fig. 2), the cross-section (Fig. 3), and the map (Fig. 4). Selected data examples are presented here, but all are available for interactive viewing in the generated digital educational data package within ArcGIS Pro, QGIS and Petrel (Table 2; Horota et al., 2022b). Individual digital files of GDCs are also available for easy inclusion in other software such as Move or Google Earth. The digital educational data package is a thematic extraction of relevant data from the Svalbox platform. The Svalbox concept comprises an open-access web portal and UNIS-internal Petrel projects, both of which are linked through a GIS-based database. Further details on the Svalbox concept are available in the literature (Betlem et al., in review; Senger et al., 2021a, 2021b, 2022a).

4. Georeferenced data containers

4.1. Terrain models and geoscientific maps

The entire study area is covered by digital elevation models (DEMs; regional ones with 20 m resolution, local ones with 2 m resolution) and

Table 1
Compilation of different data sets offered in this contribution's digital educational data package (Horota et al., 2022b). We integrate both modern data types such as DOMs and 360° images that complement and builds on pre-existing geoscientific data such as seismic, boreholes and field data.

Data type	Location	Figure	Data set DOI/ Reference to its usage
Field localities	From Festningen to East Coast (AG322, AG209, AG222 courses)	7	
Digital outcrop models	Lagmannstoppen (A)	8 A	Lord et al. (2021)
	Festningen (F)		Betlem and Senger (2022), Senger et al. (2022b)
	Värmlandsryggen (C)		Janocha et al. (2021)
	Productustoppen (D)		Senger et al. (2021d)
	Akseløya (B)		Betlem et al. (2022a)
	Midterhuken (E)	9	Betlem et al. (2022c)
	Mediumfjellet (G)	8C	Larsen (2009), https://v3geo.com/model/142
	Firkanten (H)		Betlem et al. (2022b)
	Janusfjellet (I)	15	Betlem (2021)
	Eistradalen (J)	8 B	Betlem and Rodés (2021)
360° imagery	Qualitative overview of field sites Virtual field guides	7, 10	
Terrain models and geological maps	Svalbard-wide DEM and 1:250 000 geological map	5 A	(Norwegian Polar Institute, 2014b, 2016)
Oblique aerial imagery	Qualitative overview of field sites	6, 11 E	
Bathymetry	High-resolution seafloor data, directly correlatable with onshore geology in Svalbard's fjords	11 A	Steatens Kartverket (2022), Blinova et al. (2012)
Seismic data	Good 2D seismic coverage in fjords and some of the major onshore valleys	11 B, 11C, 12	Survey map on Svalbox (www.svalbox.no/map), numerous applied studies published with interpretations
Non-seismic data (Electromagnetic, gravity, magnetic)	MT and TEM data onshore, mostly for geothermal exploration. Boat and onshore-based gravity grids. Aeromagnetic and ship-based magnetic data in Isfjorden		Beka et al. (2016), Beka et al. (2017a), Beka et al. (2017b), Dallmann (2015), Senger et al. (2013)
Borehole data (from UNIS CO2 lab boreholes and some petroleum wildcats)	Fracture data, wireline logs, digital drill core models etc.		Senger et al. (2019), Betlem et al. (2020), Ogata et al. (2014), Olaussen et al. (2019) and references therein
Published data	Structural maps, geological profiles and cross-sections	13	See section 4.10 for list of included publications
Sandbox modelling	Qualitative tools for visualizations, quantitative for research	14	Leever et al. (2011)
3D printing	Visualization tool and teaching tool, integrated with geospatial data	5 B, 5C	

(continued on next page)

Table 1 (*continued*)

Data type	Location	Figure	Data set DOI/ Reference to its usage
Geodatabase	Integration of all data sets within a spatial context	13	This paper's digital educational data package (Horota et al., 2022b)
Svalbox portal and subsurface projects	Includes a lot more data than the thematic data set presented in this article		YouTube/Zenodo (Senger et al., 2021a, 2021c, 2022b)

geological maps (mostly mapped at 1:100 000) scale. Both data sets are provided by Norwegian Polar Institute (2014a) in vector and raster formats. DEMs draped with geological maps provide an excellent starting point for identifying potential study areas, ranging from heavily tectonised rocks in western Spitsbergen to sub-horizontal structure with local fault zones in central-eastern Spitsbergen.

Other examples of basin-scale geoscientific data include regional gravity and magnetic maps (compiled by the Geological Survey of Norway; available in Dallmann, 2015 and as georeferenced images in the compiled Petrel project), lithological, surface geochemistry and Quaternary geology maps. Topographic, satellite and aerial imagery data from Norwegian Polar Institute (2022a) are also streamed into the accompanying ArcGIS and Petrel projects, allowing users to zoom in to areas of interest at the required level of detail.

4.2. Getting more out of terrain models: co-rendering with maps and 3D printing

In the context of geoscience teaching and research and developing spatial thinking skills, it is imperative to visualize features in 3D. In this context DEMs are very useful, and DEMs which are co-rendered with spatial data (e.g., tectonic maps, geological maps, satellite imagery) even more so. DEMs are available for virtually any region of the world but resolution varies. The regional DEMs for Svalbard provide 20 m resolution, but much of Spitsbergen is covered with data down to 5 m resolution. Furthermore, very high (cm-scale) resolution DEMs are present where DOMs are available. Irrespective of the resolution, DEMs can be draped with textured data and presented in 3D. This is easily done in the digital educational data package within Petrel, which has a native 3D environment (Fig. 5). Texturing can be also done using the open-source software Blender (Laporte, 2022).

3D printing is increasingly used in the geosciences (e.g., Harding et al., 2021), and is a promising approach for improving the spatial thinking of geoscience students. It is now easy and cost-effective to print single-colour DOMs, for instance of the Vardeborg mountain presented in Figs. 5A and 6D. These allow students and staff to experience "touchable topography" (Hasiuk and Harding, 2016) and be able to discuss for instance orientations of faults as viewed from different angles.

On a regional scale, we have generated a scaled model of Spitsbergen and printed it using a CraftBot 2 3D printer. The scaled (1:100.000) tiles were generated from the regional 20 m resolution DEM, using the 'DEM-to-3D' plugin for QGIS. A 3x vertical exaggeration was applied to enhance the regional topography, in particular the thick-skinned part of the WSFTB (Fig. 5B). We are also working on optimizing the projection of various geospatial data sets (e.g., geological maps, satellite imagery, DOMs) onto the 3D printed base map (Fig. 5C).

DEMs and DOMs can now be visualized or even 3D printed at virtually any scale desired. Individual 3D print tiles are constrained by the 3D printer's print size limitations, but many tiles can be merged into a regional model as illustrated in Fig. 5B. Coupled with the possibility of visualizing geospatial data such as geological maps directly onto the tiles, pre-field work planning and preparation for the visits of numerous locations affected by the WSFTB can be undertaken.

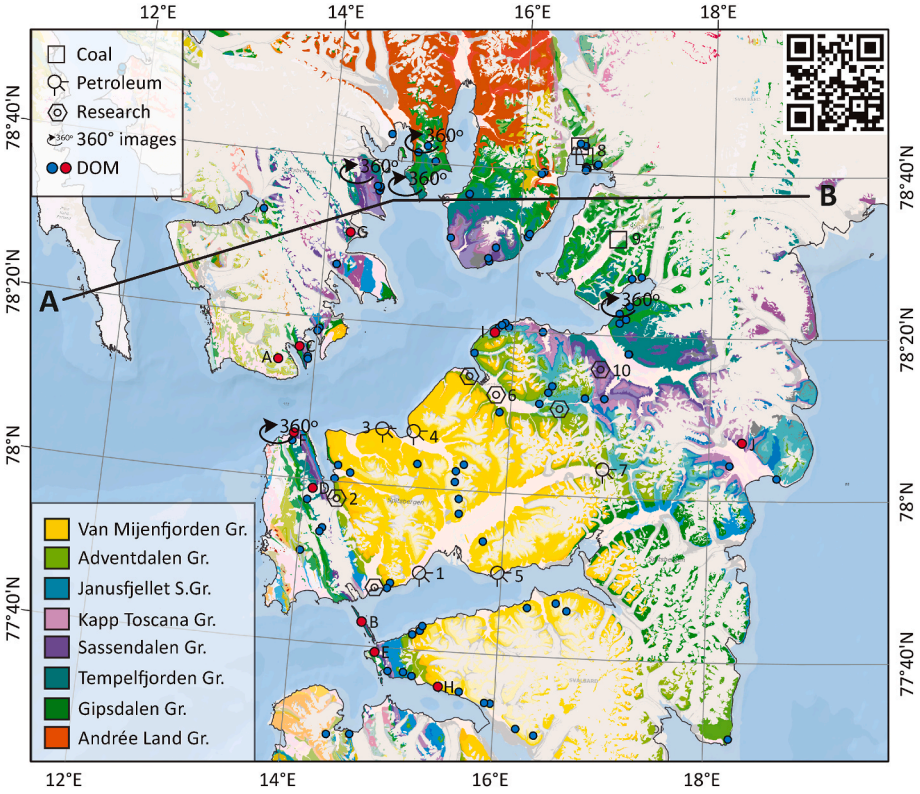

Fig. 4. Geospatial database of all georeferenced data containers provided in the interactive educational data package with this article. Refer to Table 1 for details on the data elements and their sources. The interactive data are also available on the Svalbox online portal, which includes a lot more data sets than extracted for this thematic compilation. Geological map data are courtesy of Norwegian Polar Institute (2014): https://data.npolar.no/dataset/616f7504-d68d-4018-a1ac-34e329d8ad45. Bathymetry data are courtesy of IBCAO (reference for v4).

Table 2
Overview of the compiled digital educational data package associated with this article and freely available for download via Zenodo (Horota et al., 2022b).

Main elements	Sub-elements	Formats
Pre-loaded project files	Petrel project	Petrel (.pet). Includes pre-loaded GeoTiffs of various maps, geological profiles, terrain models and well locations
	ArcGIS project	ArcGIS Includes pre-loaded GeoTiffs and profile locations
	QGIS	QGIS Includes pre-loaded GeoTiffs and profile locations
Individual data files (also for use in other software)	Digital outcrop models (see also Table 1)	.obj and Metashape, individually downloadable from Zenodo
	Figures – maps and cross sections from 24 publications	Tiffs/Jpgs for cross-sections and GeoTiffs for georeferenced maps
	Locations of cross-sections	Shapefiles
	Geological maps	Shapefile: Geological map of Svalbard (1:750000), Geological map of Svalbard (1:250000). See also, Geo Svalbard, Temadata/G_Geologi_Svalbard_S250_S750 (MapServer), Temadata/G_Geologi_Svalbard_Raster (MapServer)
	Literature	.pdfs of the articles from which maps and cross-sections are sourced
	Old aerial photos (locations)	Shapefile, see also toposvalbard.npolar.no

4.3. Remote sensing and pre-field work preparations

Prior to fieldwork in target areas, identified primarily from geological maps, outcrop conditions can be investigated using remote sensing data. A range of satellite (from Copernicus Sentinel) and aerial imagery from both summer and winter seasons covering the entire study area is accessible via the Norwegian Polar Institute (2014a). The data allow mapping of features down to the scale of driftwood (diameter ca. 20 cm) on the beaches (Fig. 6B). Such imagery is extremely useful for conducting pre-field work reconnaissance and can be used as base maps during fieldwork and post-field work mapping.

Oblique imagery is also useful for assessing field conditions. Historical oblique photographs from the late 1930s are available from the Norwegian Polar Institute (2022b) and are an important resource for planning field campaigns. Historical oblique photographs of the Grumantbyen and Vardeborg (Fig. 6D) thrusts are excellent examples of faults in the thick-skinned part of the WSFTB. Furthermore, the combination of various satellite image data types can enhance various geoscientific applications, as illustrated by the combination of DEM, satellite imagery, and geological map at Vardeborg-Festningen (Fig. 5).

4.4. Field localities and field data

The University Centre in Svalbard (UNIS) with its base in Longyearbyen at 78°N facilitates conducting field excursions to study the varied and well-exposed outcrops of Svalbard. The Arctic conditions, in particular the extreme polar night day cycles and long periods of snow cover, restrict geological fieldwork to the spring (late February-early May; access by snowmobiles) and summer (late June–September; access by boats, hiking or helicopter; Senger et al., 2021c; Senger and Nordmo, 2021). The WSFTB is best appreciated during springtime, as geological features on the west-east profile (Fig. 3) can be visited during day trips from Longyearbyen. Large-scale structures are often more discernible when there is some snow cover. Both Productustoppen (Fig. 7A) and Vardeborg (Fig. 7B) in the western part of the WSFTB near Grønfjorden are routinely visited by UNIS courses. Summer DOMs and 360° imagery (Fig. 7C) provide an additional resource during these field trips, especially if poor visibility or weather restricts access to the field sites. The increased use of digital data for quantitative studies in structural geology (Bemis et al., 2014; Vollgger and Cruden, 2016) also facilitates inclusion of DOMs from more remote locations such as Lagmannstoppen (Fig. 8A) or Mediumfjellet (Fig. 8C) north of Isfjorden (Lord et al., 2021). Structural measurements and photographs collected during fieldwork (both by UNIS researchers and from publications; e.g., Bergh and Andresen, 1990; Larsen, 2009) provide data to compare and quality-check the structural information derived from the DOMs. The field measurements can also be used to validate and compare structural measurements derived from DOMs.

4.5. Digital outcrop models

Digital outcrop models (DOMs) are digitized outcrops processed mainly using structure-from-motion (SfM) photogrammetry with many overlapping photographs as input (e.g., Westoby et al., 2012). Alternatively, DOMs can be acquired using ground- or helicopter-based Lidar scanners (Buckley et al., 2008; Rittersbacher et al., 2013), but this typically involves significant costs for both acquisition and processing.

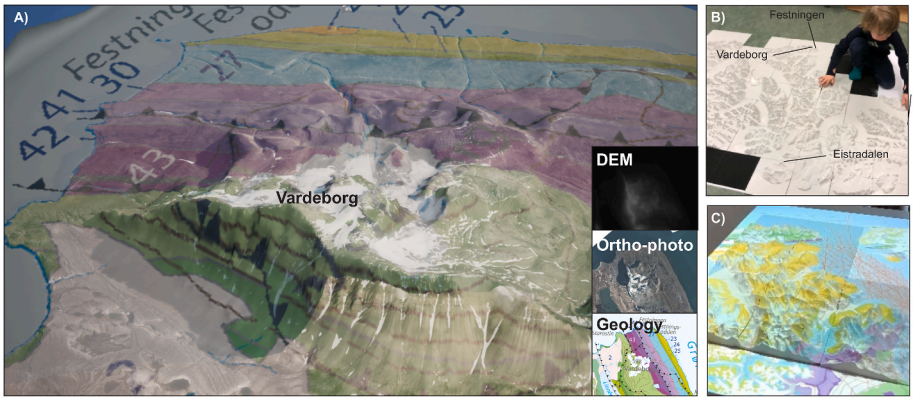

Fig. 5. A) Digital version of the Vardeborg mountain draped with a regional geological map illustrating the location of the north-east verging thrust fault. The famous Festningen section is visible in the background. The input ingredients, i.e. DEM, orthophotos and geological map, are shown as insets. B) 3D print of the Nordenskiold Land study area. The tiles were printed at 1:100.000 scale with 3x vertical exaggeration. C) Part of the model displayed with a projected geological map, illustrating the potential for maximizing the value of 3D prints by including geospatial data. The electronic whiteboard allows the interaction with DOMs while displaying regional geospatial data and is a powerful tool in both teaching and outreach. The basis of the 3D-render is the "Merged NPI-ArcticDEM Svalbard digital elevation model" (Aas and Moholdt, 2020). The textures (orthophotos, geological map) have been extracted from the data server of the Norwegian Polar Institute (© Norwegian Polar Institute, https://geodata.npolar.no).

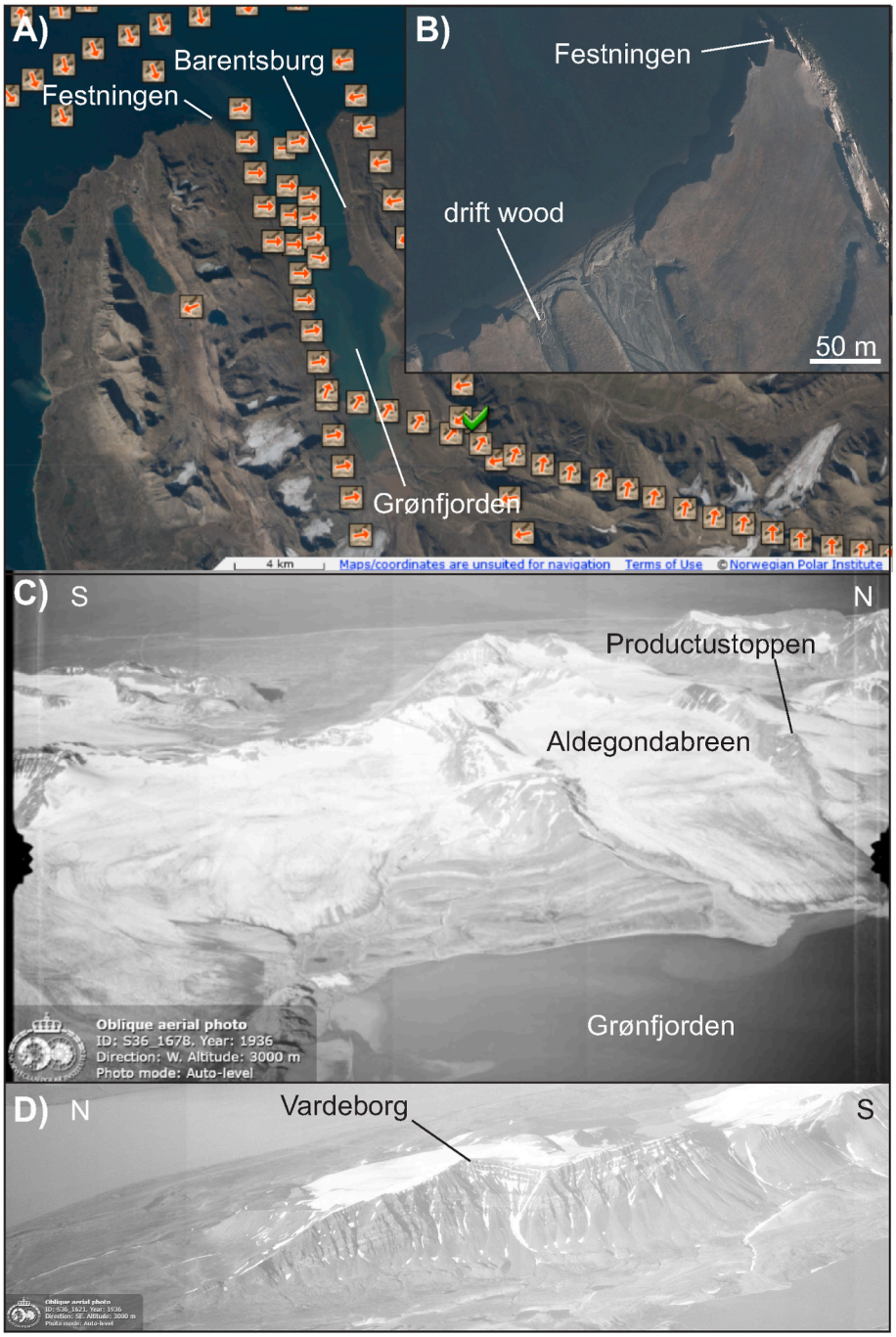

Fig. 6. Examples of pre-field preparations using oblique historic imagery and satellite imagery. A) Historical oblique imagery coverage in the Grønfjorden area in the thick-skinned part of the WSFTB. There is approximately one oblique image per km along the entire WSFTB section. B) Zoom-in of the Festningen to illustrate the detail provided by modern aerial imagery. Note the driftwood on the beach for scale. C) Historical oblique imagery of the Aldegondabreen area. D) Historical oblique imagery of Vardeborg, including a major thrust fault.

Smartphone-based Lidar scanners like the latest generation of iPhones easily generate DOMs (Tavani et al., 2022), but are presently restricted to outcrops accessible within the limited range of 5 m. Most of the DOMs freely available on the Svalbox portal are processed using drone-based photographs, covering meter to kilometer scale outcrops. The resulting high-resolution georeferenced DOMs allow quantification of orientations (e.g., fault and fracture strike/dip) and distances (e.g., fault throw, syn-sedimentary wedges near growth faults) over single DOMs from the entire WSFTB cross-section (Fig. 3).

Being 3-dimensional, DOMs have the added benefit over conventional photographs of allowing rotation of the perspective. This is especially useful when interpreting the structurally complex outcrops associated with the WSFTB (Figs. 7 and 8). Georeferencing of DOMs also eases their direct integration with other acquired geospatial data, for instance ground-penetrating radar (GPR), to "see" beyond the outcrop (Janocha et al., 2020). Selected DOMs can be integrated with the regional DEM and other geoscientific data (Fig. 8C), providing insights into the structural complexity and variability across the east-west cross-section (Fig. 3).

An example of using DOMs in structural geology is illustrated in Fig. 9 where the world-famous Midterhuken section from the WSFTB is examined. The Midterhuken DOM (Table 1; Betlem et al., 2022c) illustrates structural architecture and sequence of deformation previously interpreted by Maher et al. (1986). The uplifted metamorphic basement is exposed in the western part, unconformably overlaid by NE dipping succession that begins with the Upper Carboniferous strata (Tres. Fm. Fig. 9A). The Early Carboniferous succession is thrusted over the Late Carboniferous succession along the detachment 2, later intersected by

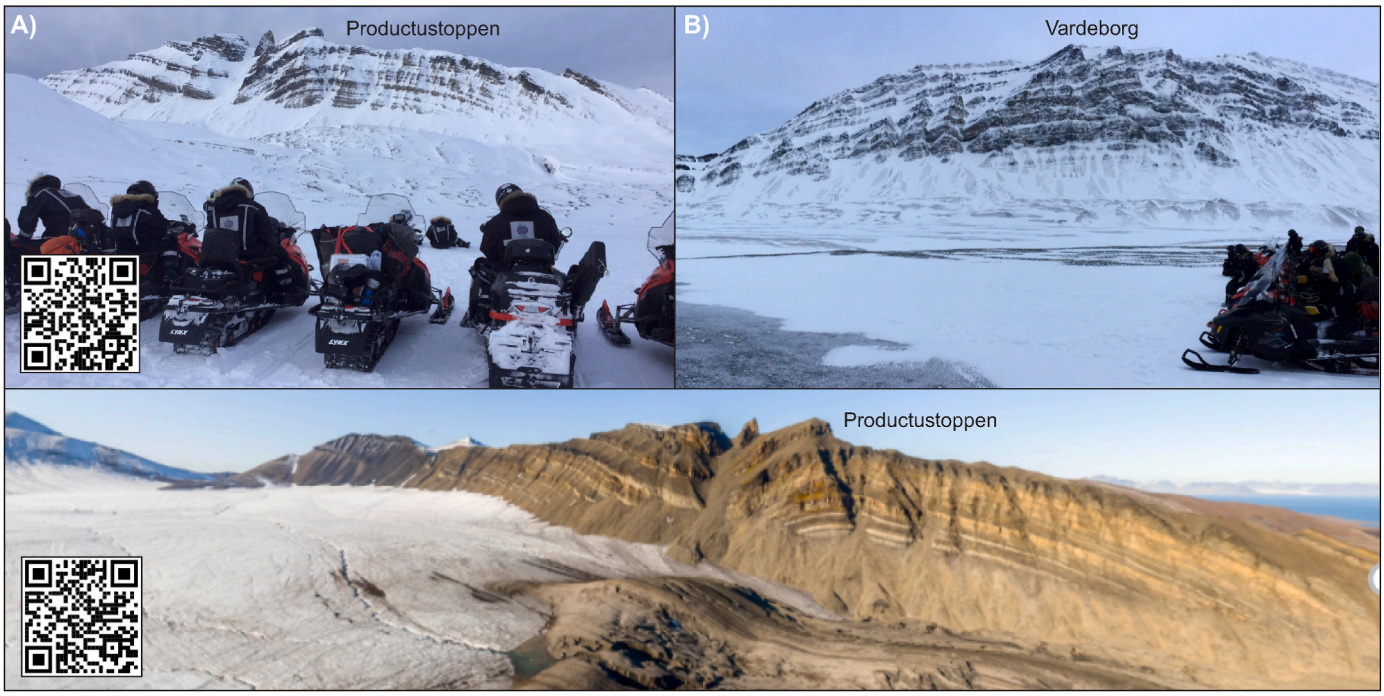

Fig. 7. Photographs from field sites visited during UNIS excursions in western Spitsbergen. A) Excursion to the WSFTB in April as part of the MSc/PhD-level AG322 course on Fold and Thrust Belts and Foreland Basins at UNIS. The QR code points to a downloadable DOM of the mountainside acquired on April 8, 2019. B) Overview of the Vardeborg thrust in April. C) Summer view of the Productustoppen mountain, acquired in August as part of the AG210 course on The Quaternary and Glacial History of Svalbard. The QR code links to a virtual field trip related to this course. AG-210 VFT, Aldegondabreen (2021).

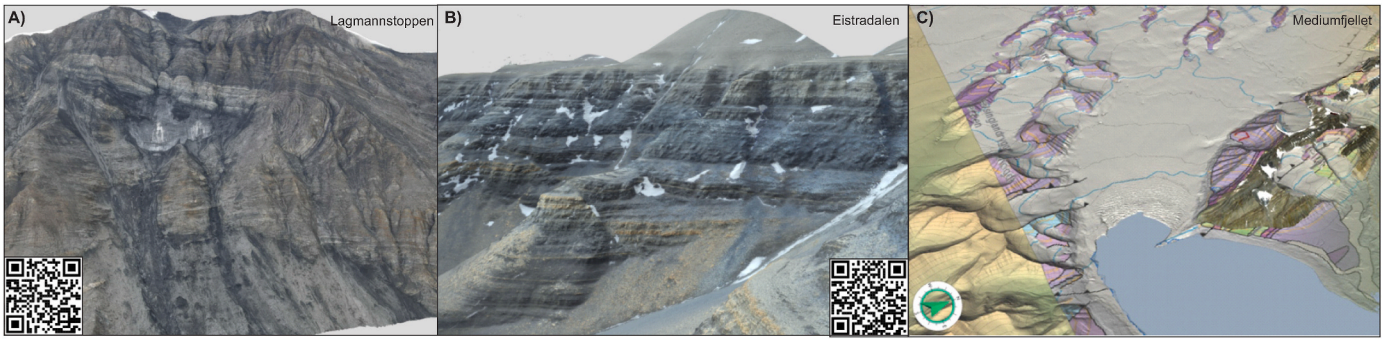

Fig. 8. Examples of two digital outcrop models from Svalbox and one from V3Geo. At Lagmannstoppen (Lord et al., 2021) in western Spitsbergen the Alkhornet Formation is heavily deformed and is a good example of thick-skinned tectonism in the WSFTB. At Eistradalen (Betlem and Rodés, 2021) in eastern Spitsbergen only the sedimentary cover is affected by faulting. The QR codes point to downloadable and interactive versions of the DOMs (also listed in Table 1, along with a number of other relevant DOMs). The Mediumfjellet model from V3Geo is placed in context by incorporating a DEM draped by a geological map and was analysed as part of the AG222 course at UNIS (Senger et al., 2021c).

thrust fault 1. The deformation along detachments 1 and 2 is related to Paleogene shortening and the formation of the WSFTB. Prior to the formation of the WSFTB this succession was intersected by Early Cretaceous HALIP-related sills whose disturbed folded and faulted pattern reflect the younger post-emplacement deformation.

Eastwards, the Upper Carboniferous-Permian succession that dips 60–70° to NE is internally deformed, highlighted by slip surface 3 located in at the onset of gypsum-rich and poorly exposing the Early Permian Gipshuken Formation (Maher et al., 1986). This level of deformation corresponds to the regional lower detachment presented in Fig. 2. The middle detachment from Braathen et al. (1999) is marked at Midterhuken as Midterhukbreen detachment (See 4 in Fig. 9), expressed along the base of the organic-rich, mudstone dominated Bravaisberget Formation of Middle Triassic age. The underlying succession is unfolded in contrast to the overlying thigh and disharmonic folds. The overall movement indicated by offset on the intrusion as well as pattern of faults and floods is hanging-wall- down (see the Midterhuken evolution in Maher et al., 1986).

The Midterhuken model nicely illustrates the principle of parasitic folds. The Middle Triassic succession is forming a fold with smaller-scale disharmonious parasitic folds (Fig. 8g). The detailed analysis of the Midterhuken digital outcrop model allows to illustrate M-folds in the middle of the anticline and Z-folds in the NE limb of the anticline (Fig. 9H).

Notably, the analyses presented for Midterhuken in Fig. 9 were conducted using only the material in the digital educational data package associated with this article – the DOM itself and the relevant published literature. As such, the presented case study serves as an example for how others can actively use the digital educational data package (Horota et al., 2022b).

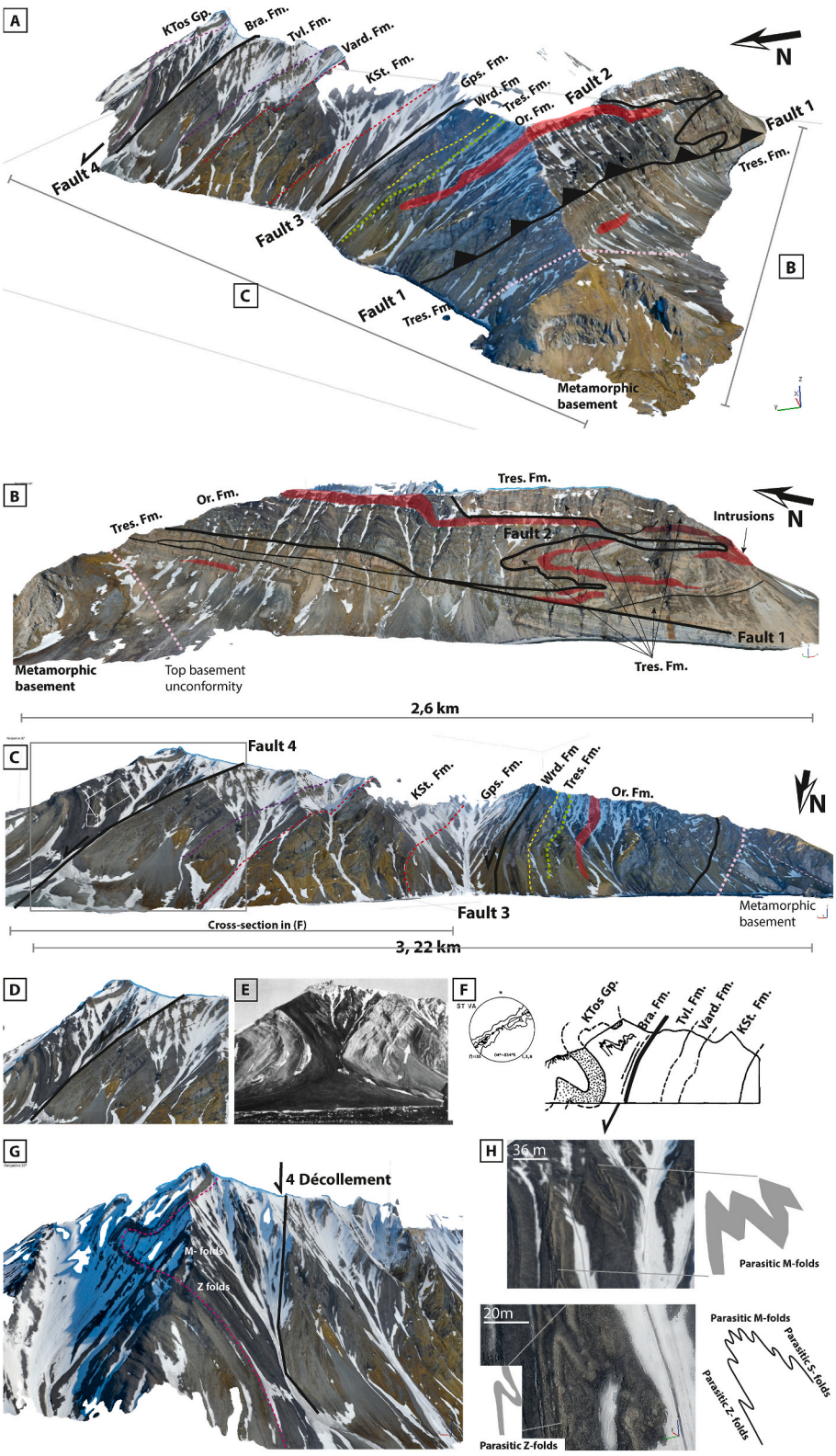

Fig. 9. A-c Visualization of Miderhuken digital outcrop model with highlighted interpretation of major dislocations and stratigraphic units. Major faults and detachments are marked with numbers 1–4 and illustrated with bold black lines (interpretation from Maher et al., 1986; 1- Midterhuken décollement (Senger et al., 2019); 2- Bravaisknatten fault; 3- base Gipshuken Formation slip surface; 4- Midterhukbreen detachment fault zone). Other faults and thrust are market with thin black lines. Top basement and mid-Carboniferous unconformities are marked with dashed pink and green lines respectively. Remining stratigraphic boundaries are marked with dashed yellow-red coloured lines. Ors. Fm: The Lower Carboniferous Orustdalen Formation (sandstones and coaly mudstones); Tres. Fm: The Upper Carboniferous/Early Permian Treskelodden Formation (sandstones, conglomerates and carbonates); Wrd. Fm: The Upper Carboniferous/Early Permian Wordiekammen Formation (carbonates); Gps. Fm: Gipshuken Formation (gypsum/anhydrites and limestones); KSt. Fm: The Upper Permian Kapp Starostin Formation (carbonates, spiculites; Tvl. Fm: Lower Triassic Tvillingodden Formation (mudstones and sandstones); Vard. Fm: Lower Triassic Vardebukta Formation (mudstones and sandstones); Bra. Fm: Middle Triassic Bravaisberget Formation (mudstones); KTos Gp: Kapp Toscana Group (sandstones, mudstones and conglomerates); d-f illustrate the digital outcrop model of Midterhukbreen detachment (4) along with field photo, stereo plot, and cross-section from Maher et al. (1986); g-h shows the parasitic Z and M-folds developed within middle-Triassic succession. (For interpretation of the references to colour in this figure legend, the reader is referred to the Web version of this article.)

4.6. 360° imagery and drone photographs

While not as quantitative as DOMs, 360° imagery (still photographs and videos; also called photospheres) provide an excellent overview of a field area. These images allow the visualization of all the context that is situated around the nodal point (image acquisition point), centered on the position of a camera, that through specific software can be visualized as an interactive panoramic image. Georeferenced 360° images can be acquired from the ground or in bird's-eye view mode with drones.

The 360° images can be organized in a logical sequence in software or web-based platforms as virtual field guides with contextual information (Fig. 10; The Paleogene Transpression (2022)), providing geoscientists the opportunity to interact with the data through the ability to pan the camera while zooming in and out, changing the viewer

Fig. 10. Usage of 360° imagery for providing an overview of the field area and facilitating story-building using the VR Svalbard platform. A) 360° from a drone illustrating the Kapp Linne region – the image displays info, satellite map, custom map, figures, and 3D models anchored on the landscape. The start site of the Paleogene transpression virtual field trip is accessible thought (The Paleogene Transpression, 2022). B) Highlight of the custom geological map with interactive 360° imagery waypoint of the Festningen site. C) Festningen location drone overview 360° showing the transitional hotspot to another location. D) Kapp Starostin location with geological map and information.

perspective, essentially allowing them to explore a place in 360° on a desktop computer or seamlessly and immersively by using 3-axis movement VR headsets (see Fig. 11).

The contextual information is the digital geological educational materials that guide the virtual experience as interactive links embedded into each photosphere. The user than can access the materials (images, DOMs, geologic and topographic maps, satellite imagery, text, publish papers, etc.) related to each given photosphere connecting field related information to the landscape/outcrop.

4.7. Multibeam bathymetry

The near-shore geology in Svalbard's fjords such as Isfjorden is directly correlated to the onshore geology and the enhanced data coverage in the fjords (especially 2D seismic and 3D multibeam data) provide important constraints on the tectonic architecture of Svalbard. The seafloor in Svalbard's fjords is mapped at 5 m resolution, which is a higher resolution than the regional onshore DEMs. The near-complete coverage allows the mapping of m-scale pockmarks testifying past fluid flow (Roy et al., 2015, 2019), positive ridges related to WSFTB thrust faults (Blinova et al., 2012, 2013) or sub-cropping igneous intrusions (Senger et al., 2013). 3D multibeam bathymetry is also useful to directly tie the seafloor morphology to the 2D seismic grid, and to conduct direct onshore-offshore correlations for geological seafloor mapping.

4.8. Seismic data

A relatively dense 2D seismic grid is available in Isfjorden comprising both industry (acquired mostly in the late 1980s and early 1990s as part of petroleum exploration) and academic surveys (Fig. 12; Anell et al., 2014; Blinova et al., 2013; Bælum et al., 2012; Eiken, 1994; Senger et al., 2013). Onshore Spitsbergen, seismic lines are restricted to major valleys and some glaciers and have mostly been acquired using snowstreamers

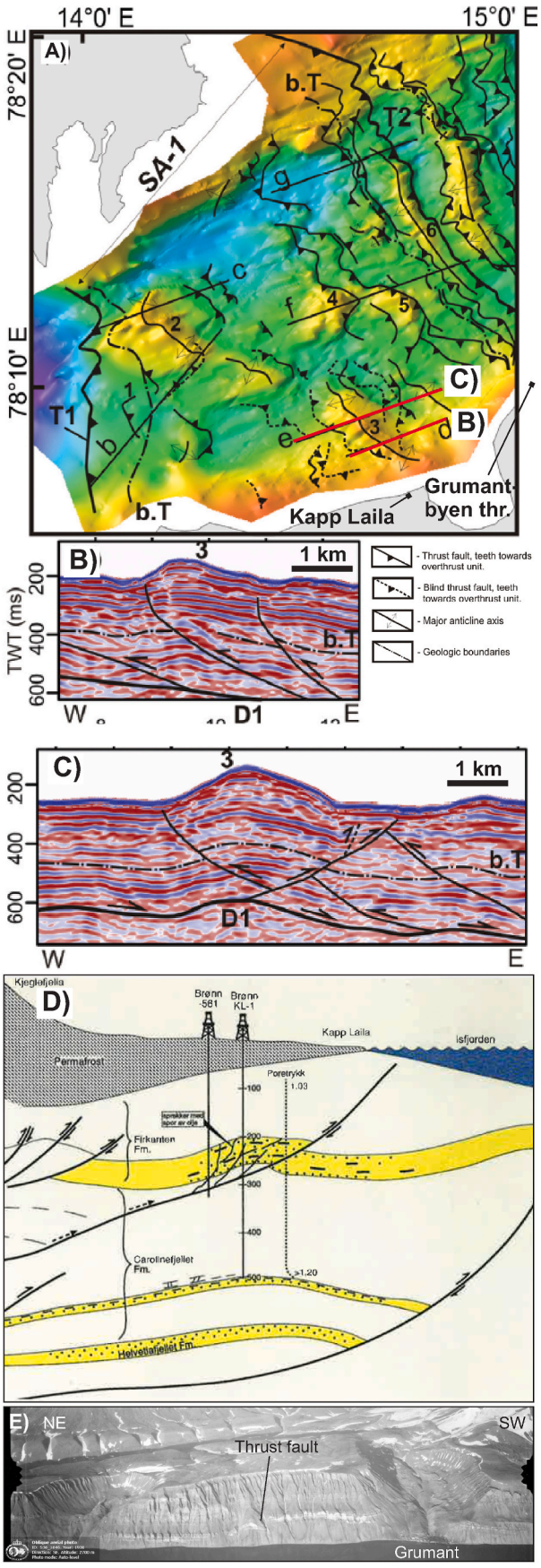

(caption on next column)

Fig. 11. Thrust faults related to the WSFTB as identified on various datasets in Isfjorden, including multibeam bathymetry, 2D seismic, borehole and outcrop data. A) Interpreted multibeam bathymetry in Isfjorden illustrating the outcropping thrust faults on the seafloor, from Blinova et al. (2012). B) and C) 2D seismic profiles crossing the fault scars on the bathymetry and illustrating their overall geometry and structure, including the tendency of thrust faults to sole out in the major decollement layer D1. D) Cross-section across the Kapp Laila exploration borehole (see A) for location). The well targeted anticlines set up by such thrust faults. Figure from SNSK, published by Brugmans (2008). E) Oblique aerial image of a well-exposed thrust fault at Grumantbyen.

(Eiken et al., 1989). The high seismic velocity of Svalbard's compacted sediments (generally exceeding 4 km/s; Bælum and Braathen, 2012) reduces seismic resolution and also introduces challenges when processing out the very strong seabed reflector on the offshore data. Nonetheless, seismic data, particularly when integrated with onshore geology and multibeam bathymetry, can both constrain the overall subsurface structures (Bælum et al., 2012), map thrust faults (Blinova et al., 2012, 2013) or quantify fault zones.

4.9. Non-seismic geophysics (electromagnetic and potential field data)

The entire study area is covered by regional gravity and aeromagnetic data (Dallmann, 2015). Locally ship-based magnetic data, acquired during the Svalex seismic campaigns, complement these regional datasets and facilitate the mapping of magnetic igneous intrusions (Senger et al., 2013). More recently, a number of magnetotelluric (MT) profiles were acquired as part of geothermal exploration of Svalbard, including in Adventdalen-Sassendalen (Beka et al., 2016) and Brøggerhalvøya in the thick-skinned part of the WSFTB (Beka et al., 2017a). Joint inversion of MT and transient electromagnetic (TEM) data in Adventdalen focused on the reservoir-caprock succession of the Longyearbyen CO_2 lab project (Beka et al., 2017b). The same study also integrated resistivity from the electromagnetic data sets to the acoustic impedance from seismic data by spatially correlating the two independent profiles sensing different physical properties but over the same subsurface.

4.10. Borehole data

Eighteen petroleum exploration boreholes were drilled in Svalbard from 1961 to 1994 (Senger et al., 2019) and many of these are located within the Central Spitsbergen Basin (Fig. 4). The penetrated strata show evidence of thrusting (leading to both repeated and missing strata) and enhanced fracturing in shale-dominated intervals. Five research boreholes near Longyearbyen drilled for CO_2 storage penetrate the uppermost decollement within Late Jurassic shale-dominated strata, which has caused considerable drilling challenges due to clay swelling (Braathen et al., 2012; Olaussen et al., 2019). Finally, a fully cored 1.1 km deep research borehole drilled at Sysselmannbreen and tied to a 2D seismic grid provides insights into the infill of the foreland basin reflecting its tectonic evolution (Johannessen et al., 2011; Johansen et al., 2011).

4.11. Published maps, profiles and geological context

Numerous publications provide detailed maps and geological cross-sections across parts of the WSFTB (Bergh and Andresen, 1990; Bergh et al., 1997; Blinova et al., 2009; Braathen et al., 1995; Dallmann, 2015; Johansen et al., 1994), which were initially compiled in Bergh et al. (1997). These maps (as GeoTiffs) and profile locations (as Tiffs in the correct place) are digitized and compiled in the digital educational data package (Horota et al., 2022b). Furthermore, the georeferenced maps and profiles are integrated in a ArcGIS (Fig. 13A), QGIS and Petrel (Fig. 13B and C) projects along with all available GDCs. The digital educational data package tied to this article includes maps and profiles

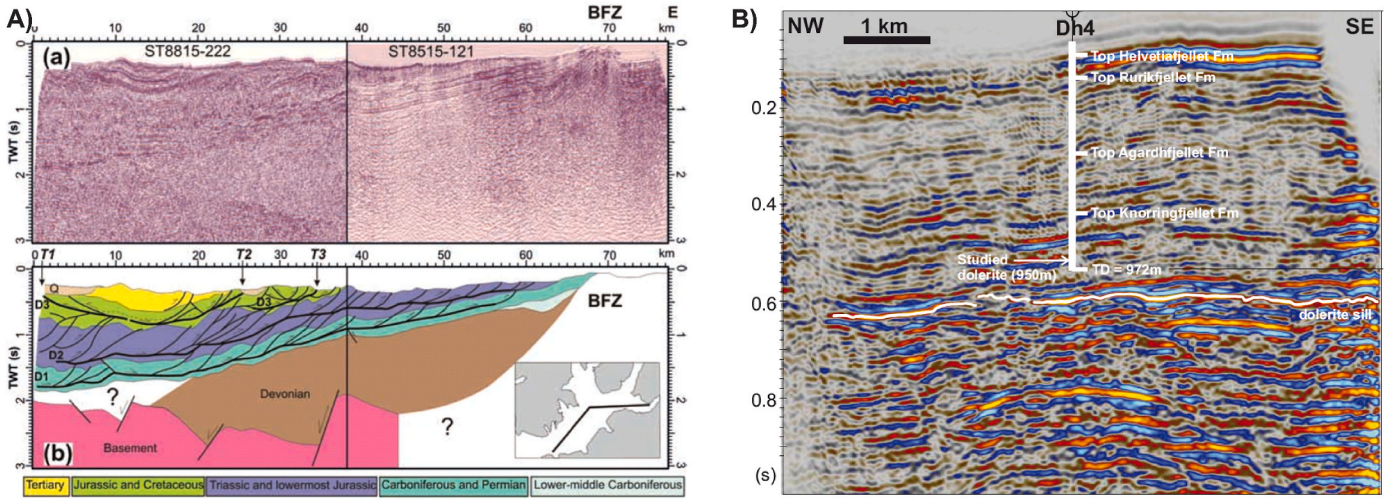

Fig. 12. Examples of published offshore (A) and onshore (B) seismic data, both provided in the electronic data compilation within this contribution. The offshore regional profile from Blinova et al. (2013) highlights the major decollement zones and the offshooting thrust faults. The onshore example in Adventfjorden, from Senger et al. (2014a), links the deepest borehole of the CO_2 lab project with a 1988 2D seismic profile collected for petroleum exploration. An Early Cretaceous sill is interpreted on the profile and confirmed by field studies.

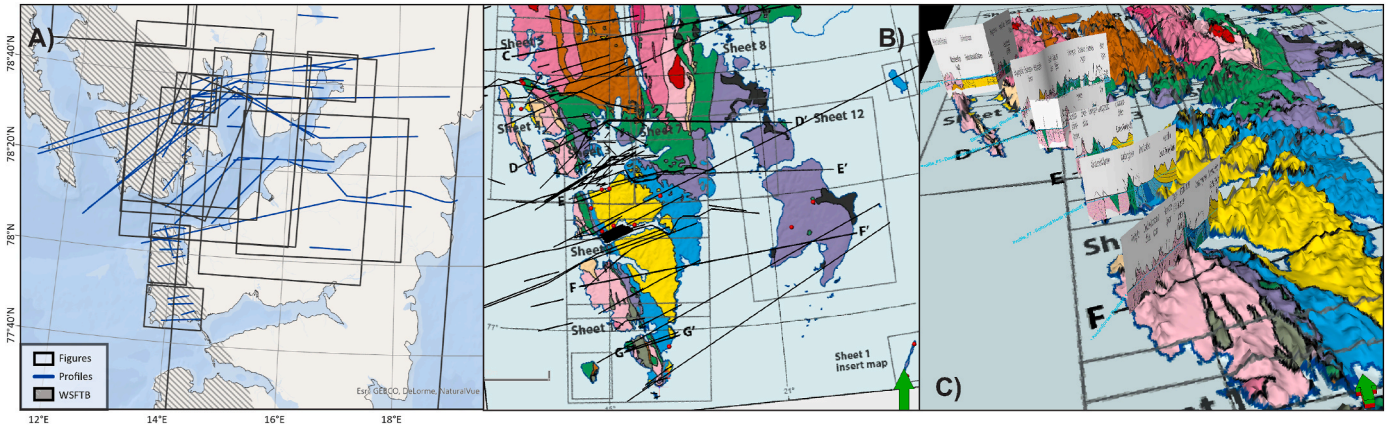

Fig. 13. Data integration in GIS (A) and Petrel (B and C), illustrating the integration of georeferenced data containers within the digital educational data package. A) Screenshot of the digital educational data package, illustrating selected published maps and all the digitized published profiles within the ArcGIS environment (also applicable for QGIS). B) Screenshot of the available profiles (black lines) in Petrel, displayed on a georeferenced geological map of Svalbard.) C) Screenshot from Petrel, where selected regional geoscience profiles crossing the West Spitsbergen Fold and Thrust Belt (from Dallmann, 2015) are directly integrated with a geological map draped on the regional terrain model.

from numerous publications (Bergh and Andresen, 1990; Bergh et al., 1997; Blinova et al., 2012, 2013; Braathen et al., 1995, 1999; Maher et al., 1995).

4.12. Sandbox modelling

Many of the large-scale structural elements, such as rift basins and fold and thrust belts, discernible in the field can be simulated using a sandbox model, and these are routinely used for qualitative demonstrations in UNIS courses (Fig. 14). The sandbox models, often conducted in the polar night before the fieldwork is undertaken, allow students to observe the process of fault development from faults nucleation to cessation, in both compressional and extensional settings. Furthermore, sandbox modelling exercises contribute to ensuring a baseline for students with diverse previous geological backgrounds. This is especially important at UNIS where students come from numerous Norwegian and international home universities with different geoscience study programs. The most important learning objective ascribed to performing sandbox models is based on the four-dimensional character of the experiments. This allows us to introduce and discuss with students the geological time scale and observe dynamic process of formation of geological structures, not just the final effect which can be seen in the field. The second objective of the sandbox is to discuss the spatial scale of the geological structures in nature versus on maps and cross-sections. In addition, cutting the sandbox models at the end of the experiments allows students to visualise intersection of the structures that can be observed at different angles.

The development of the WSFTB is also simulated through quantitative sandbox studies, which are also available in the digital educational data package. One of the key papers is by Leever et al. (2011), who simulated the structural evolution of the WSFTB under transpressional boundary conditions using an analogue model of sand hosting three silicon layers as that simulate regional detachments. The modelling defines a three-step evolution starting with a transpressional fault-controlled ridge along the transform, or positive flower structure, with subsequent lateral spreading as a localized fold-thrust belt above silicon detachments.

Fig. 14. Illustration of using a qualitative sandbox model during structural geology teaching at UNIS. A) Students of the AG209 course on the "Tectonic and Sedimentary History of Svalbard" discussing a compressional experiment using the UNIS in-house Svalbox sandbox model. B) Detailed view of some of the generated compressional features.

4.13. Integration of georeferenced data containers and applications for re-visiting structural evolution of Spitsbergen

This article is complemented with a digital educational data package (Horota et al., 2022b), listed in Table 2, that integrates most of the elements described in sections 4.1-4.12 and listed in Table 1. All data are pre-loaded into Petrel and ArcGIS (both licensed software, but with free (Petrel) and discounted (ArcGIS) academic licenses available for many academic institutions) and QGIS (open-source software). GDCs are integrated by their position within the basin. Petrel is a truly 3D platform, and therefore includes geological profiles and seismic data that can be visualized in 3D windows along with terrain data (Figs. 5 and 13C). The ArcGIS and QGIS projects (Fig. 13A) include the position of all profiles and 2D data but require visualizing the subsurface profiles as separate images. Locations of DOMs are included in Petrel, ArcGIS and QGIS through Svalbox web map services but cannot at present be visualized within either of them. For this reason, visualization of DOMs using SketchFab or V3Geo (for selected Svalbox models) is feasible using the metadata provided with the DOMs as used online on the Svalbox webpage. Users can also use licensed (e.g., Metashape, LIME; Buckley et al., 2019) or open source solutions (e.g., SketchFab, potree, Unity, CloudCompare; Nesbit et al., 2020) to display, interact and interpret the DOMs and associated point cloud data. The interpretation of Midterhuken (Fig. 8) was conducted in Metashape.

The digital educational data package builds on extensive previous studies on the WSFTB. Through geospatial integration of this all data related to this geological event with regional (gravity, magnetic, seismic, DEM etc.) and site-specific (DOMs, 360° imagery, field data etc.) data sets allow for clearer definition of knowledge gaps and further research. Quantitative structural restorations in 2D and 3D, for instance, are more easily attempted when building on the framework of the presented electronic data package. Understanding both the along-strike differences in deformations styles, shortening and sequence of deformation within the WSFTB can be complemented by quantitative analyses on the presented DOMs from various segments of the orogenic belt. One example of quantitative interpretation of a DOM is provided for Midterhuken (Fig. 9).

5. Discussion

5.1. Data integration and story-building

In this study we have compiled and integrated a wide range of georeferenced data sets of relevance for understanding the WSFTB and its associated foreland basin. DOMs (Fig. 8) are particularly useful to illustrate the structural complexity across the basin, from thick-skinned tectonics in the west (e.g., Lagmannstoppen; Lord et al., 2021) to thin-skinned tectonics in the east (e.g., Eistradalen; Betlem and Rodés, 2021). However, the power of DOMs increases significantly when seen in the context of regional geology.

In Svalbard, this is achieved through the Svalbox database, which integrates DOMs with maps (geologic, topographic, paleogeographic, gravity/magnetic etc.), subsurface profiles, seismic, terrain models, bathymetry and published logs (Betlem et al., in review; Senger et al., 2021a, 2021c). Svalbox is accessible both through location- and data type-based Petrel projects (available at UNIS, with a thematic Petrel project in the digital educational data package (Horota et al., 2022b)) and through the archipelago-wide data portal at www.svalbox.no (available everywhere).

There are a number of repositories of DOMs available, including e-Rock (Cawood and Bond, 2019), V3Geo (Buckley et al., 2022), MOSIS (Gonzaga et al., 2018) and virtual Australia (Roach, 2019), but none truly integrate DOMs with complementary data as conducted in Svalbox. Furthermore, DOMs from Svalbox are fully available for download and re-use, including raw input imagery, processed point clouds, models and the Metashape project files (Table 1; Betlem, 2021; Betlem and Rodés, 2021;; ; Betlem and Senger, 2022; Janocha et al., 2021; Lord et al., 2021; Senger et al., 2021d).

In-context data integration extending far beyond DOMs facilitates "story-building". Through the use of Virtual Field Trips (VFTs) implemented as StoryMaps, both teachers and students at UNIS have been able to make the amazing geology of Svalbard come alive. VFTs often embed both DOMs and complementary geoscientific data to provide thematic excursions based on data available in Svalbox. Fig. 10 illustrates another approach to develop VFTs, using 360° imagery as building blocks for the thematic VFT made specifically for the WSFTB. As demonstrated in this contribution, the Svalbox concept and its rich underlying database can also generate meaningful integrated data resource packages for training (both academic and industry) and research.

5.2. Spatial and 3D thinking

The presented digital educational data package makes use of DOMs, 360° imagery, and 2D integrated data to remotely illustrate, and provide virtual extended access to the complex geology of the WSFTB. These 3D digital representations were also selected to integrate directly with the AG-209 ('The Tectonic and Sedimentary History of Svalbard', 15 ECTS Bachelor-level course) and AG-222 ('Integrated Geological Methods: From Outcrop to Geomodel', 15 ECTS Bachelor-level course) courses, held during the spring semester at UNIS (Senger et al., 2021a).

This dataset provides an excellent opportunity to assist in 3D thinking by allowing multiple perspectives of the same features. As illustrated in Fig. 15, a thrust fault with an associated fault-propagation fold exposed at Janusfjellet can be explored from a limitless number of vantage points and magnifications. Furthermore, structural measurements of bedding and fault planes extracted from the DOM can be used to generate surfaces, as routinely used in geomodelling. By generating

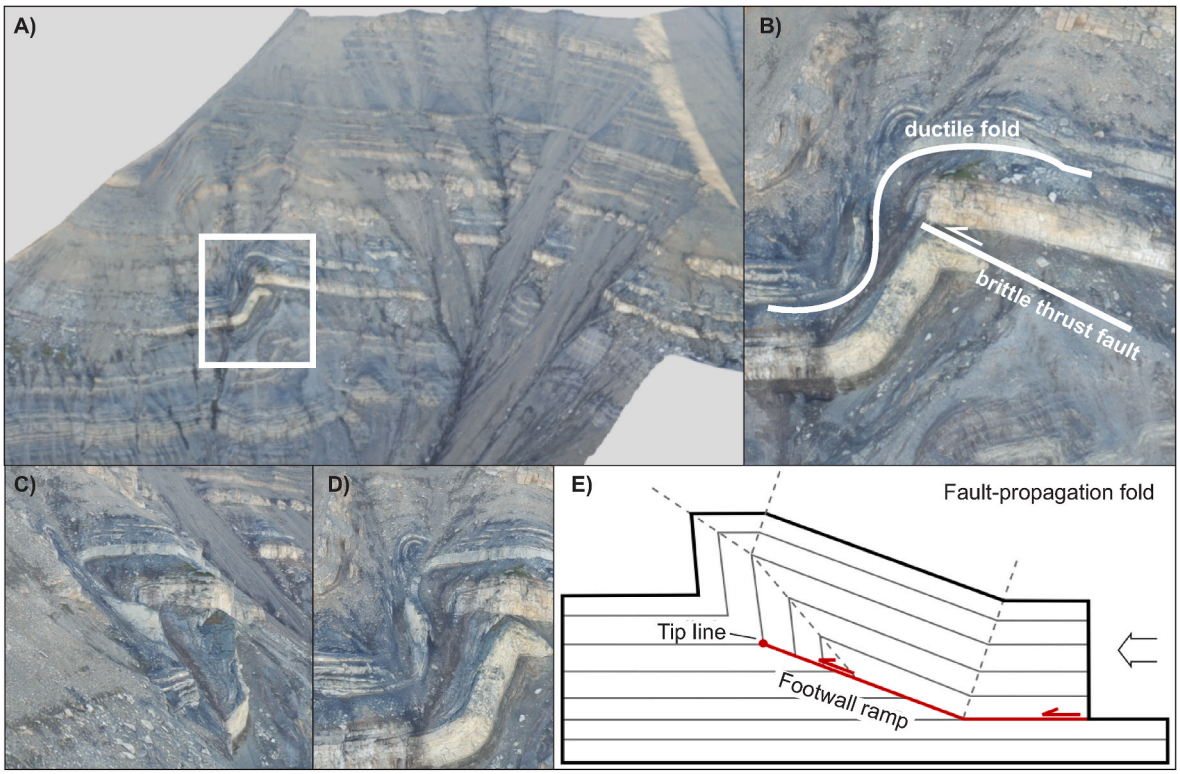

Fig. 15. Screenshots of the Janusfjellet digital outcrop model (Betlem, 2021), from a number of perspectives (B–D). The white rectangle illustrates the main point of interest where a Paleogene thrust faut is cutting the Early Cretaceous sandstone. The geologist is referred to the digital version of the DOM for scale and orientation. E) is a schematic representation of the fault-propagation fold seen in this outcrop.

surfaces of various features and co-visualizing these with the DOMs, geologists can infer the interactions of various features, such as presented fault-propagation fold at Janusfjellet (Fig. 15) and the decollement zone located stratigraphically below.

In contrast, until recently the students of the aforementioned UNIS courses needed to envision the three-dimensional shape of mountain-scale 3D-structures, such as faults and folds, from the overview points. This allows semi-two-dimensional perception of observed structures at the one fixed angle. The cold Arctic fieldwork conditions provide an added challenge, with limited time available at each outcrop. The use of DOMs allows to change the perspective, zoom in and out from the structures and rotate them to avoid interpretations misled by sub-optimal observation angles. This is particularly important when analyzing fault displacement. For instance, extensional faults may sometimes appear contractional when observed at a high angle to the fault plane. Rotation allows for observations along the fault plane, decreasing the chance for misinterpretation.

Every time geoscientists want to acquire, represent, manipulate, or discussion about geological structures, processes, or phenomena in space their spatial thinking skills are exercised (Kastens et al., 2009). Digital or virtual outcrop models manipulation can improve a geologist's spatial thinking skills when compared with other 2D representations, such as maps and cross-sections (Bond and Cawood, 2021; Carbonell Carrera and Bermejo Asensio, 2017). Meanwhile, the 360° imagery allows the visualization of the geological context surrounding an image's nodal point, centered on the position of a drone, mobile app user, or 360° camera.

In geology, the observer's perspective is commonly implicit in the images obtained, and in interpretive schemes of the landscapes. However, using drone-based 360° aerial images taken from different points of view allow the observation of the landscape with an advantageous and sometimes wider field of view, which when combined with DOMs and 2D integrated data representations such as geological or seismic profiles can enhance the learning of spatial thinking skills even further.

5.3. Perspectives on field learning: from hand-sample to basin-scale

Fieldwork in geosciences is becoming transformed by an increase in the use of digital technologies in field courses to such an extent that students cannot rely only on observations done while in the field to develop an understanding of the geological setting under study (Lundmark et al., 2020).

Field learning activities are undoubtedly important and crucial in educating the next generation of structural geologists. However, we can no longer ignore the benefits of also exposing students to photorealistic 3D digital representations of outcrops and landscapes when considering a multi-scale investigation of a geological context, such as the WSFTB presented here. Deciphering such events will always require strong temporal and spatial thinking skills from the students, but it does not mean that this knowledge can only come from physical fieldwork experiences. On the contrary, these key skills in geoscience education (Kastens et al., 2009) can be overcome through classroom exercises also using digital field representations. By combining the advantages that both traditional fieldwork (appreciation of scales, sampling potential, high-resolution studies, field discussions) and digital (perspective, access the inaccessible, quantitative measurements) settings provide, structural geologists can benefit from both. Bird-eye view 360° images and DOMs acquired by drones can be visualized before leaving for the field and following fieldwork. 360° imagery offers advantageous points of view over meter to kilometer-scale outcrops, while the DOMs or Digital Sample Models (DSM; Betlem et al., 2020) provide three rotational axes to explore them in any direction students like and conduct quantitative analyses. The entire experience with these digital tools can be enhanced when visualized in immersive Virtual Reality (VR) environments using VR headsets. When integrated as part of a virtual field trip (VFT; Horota et al., 2022a; Pugsley et al., 2021).

VFTs are not, in our opinion, a replacement for fieldwork, but provide significant added value in both the pre-field and post-field stages. In some cases where economic, social, or environmental reasons prevent traditional fieldwork, VFTs may also be used without a fieldwork component. According to Gilley et al. (2015), VFTs should not be used to replace traditional field trips but to introduce students to fundamental skills needed to understand their environment prior to going into the field.

At UNIS, VFTs are developed by and for students to experience the field in pre- and post fieldwork exercises (Senger et al., 2021c). By doing so, students are better prepared for the field setting. The high Arctic field setting can be overwhelming, especially for students who experience it for the first time. When brought out in the field, their attention might be overly focused on familiarizing themselves with a new geological and physio-geographic setting, and the learning process gets hampered as a result. Digital tools aid the students in overcoming this initial barrier by letting them "virtually visit" the field sites beforehand and thereby better prepare them for the field.

6. Summary and conclusions

In this contribution we have integrated a range of georeferenced geoscientific data in a single digital educational data package (Horota et al., 2022b) to illustrate the tectonic evolution across a fold-and-thrust belt. As a case study we use the high Arctic West Spitsbergen Fold-and-Thrust Belt. We actively use the Svalbox geoscience portal to extract relevant surface and subsurface data sets that are of most relevance and present these data as a set of georeferenced data containers in the overall spatial setting of the orogenic belt and associated basin. We highlight the use of digital outcrop models to illustrate the structural features associated with the WSFTB in both its thick-skinned and thin-skinned domains. Furthermore, we discuss the implications of using such digital integrated tools in geoscience education. We discuss the concepts of scale (from hand sample to basin-scale), in-context data integration and spatial thinking associated with the digital outcrop models.

Author contributions

RKH - Conceptualization, Writing – original draft, Methodology, Formal analysis, Data curation. KS – Conceptualization, Writing – original draft, Project administration, Visualization, Funding acquisition, Supervision. NR - Data curation, Writing – review & editing, Visualization, Formal analysis. PB - Data curation, Writing – review & editing, Visualization, Formal analysis. ASS - Visualization, Formal analysis, Writing – review & editing. MJ - Funding acquisition, Supervision, Writing – review & editing. DK – Visualization, Writing – review & editing. AB - Writing – review & editing

Declaration of competing interest

The authors declare that they have no known competing financial interests or personal relationships that could have appeared to influence the work reported in this paper.

Data availability

Data in Zenodo, see manuscript for details.

Acknowledgements

This study has been largely financed by the Norwegian Centre for Integrated Earth Science Education iEarth (Norwegian Agency for International Cooperation and Quality Enhancement in Higher Education grant #101060). Additional funding was provided by the Norwegian CCS Research Centre (NCCS; industry partners and the Research Council of Norway grant #257579) and Aker BP AS. The Svalbox platform is co-financed by the University of the Arctic, the Research Council of Norway (through a Svalbard Strategic Grant; grant #331679) and the University Centre in Svalbard. We appreciate the academic licenses of Petrel, the Blueback Toolbox, Metashape and Unreal engine provided by Schlumberger, Cegal, Agisoft and Epic Games, respectively. Similarly, we appreciate the open-source software providers, notably QGIS and Blender. We appreciate technical discussions and data provision from our close colleagues, notably Tom Birchall, Sten-Andreas Grundvåg, Snorre Olaussen, Anders Dahlin, Anna Sartell, Tereza Mosočiová, Gareth Lord, Mark Furze and Julian Janocha. Sofie Kolsum and Niklas Schaaf digitized and georeferenced all the profiles in Petrel. Finally, we thank an anonymous reviewer and A. R. Cruden for their constructive feedback on an earlier version of the manuscript.

References

Aas, H.F., Moholdt, G., 2020. In: Institute, N.P. (Ed.), Merged NPI-ArcticDEM Svalbard Digital Elevation Model.

Anell, I., Braathen, A., Olaussen, S., 2014. The triassic-early jurassic of the northern Barents shelf: a regional understanding of the longyearbyen CO_2 reservoir. Norw. J. Geol. 94 (2–3), 83–98.

Atchison, C.L., Feig, A.D., 2011. Theoretical perspectives on constructing experience through alternative field-based learning environments for students with mobility impairments. Qualitative inquiry in geoscience education research 44 (2), 11–21.

Atchison, C.L., Libarkin, J.C., 2013. Fostering accessibility in geoscience training programs. Eos, Transactions American Geophysical Union 94 (44), 400-400.

Baker, M., 2006. Status Report on Geoscience Summer Field Camps. American Geological Institute, Washington, DC. Report GW-06.003: 8.

Bælum, K., Braathen, A., 2012. Along-strike changes in fault array and rift basin geometry of the Carboniferous Billefjorden Trough, Svalbard, Norway. Tectonophysics 546–547, 38–55.

Bælum, K., Johansen, T.A., Johnsen, H., Rød, K., Ruud, B.O., Braathen, A., 2012. Subsurface geometries of the Longyearbyen CO_2 lab in Central Spitsbergen, as mapped by reflection seismic data. Norw. J. Geol. 92, 377–389.

Beka, T.I., Smirnov, M., Birkelund, Y., Senger, K., Bergh, S.G., 2016. Analysis and 3D inversion of magnetotelluric crooked profile data from central Svalbard for geothermal application. Tectonophysics. https://doi.org/10.1016/j.tecto.2016.07.024.

Beka, T.I., Bergh, S.G., Smirnov, M., Birkelund, Y., 2017a. Magnetotelluric signatures of the complex tertiary fold–thrust belt and extensional fault architecture beneath Brøggerhalvøya, Svalbard. Polar Res. 36 (1), 1409586.

Beka, T.I., Senger, K., Autio, U.A., Smirnov, M., Birkelund, Y., 2017b. Integrated electromagnetic data investigation of a Mesozoic CO 2 storage target reservoir-caprock succession, Svalbard. J. Appl. Geophys. 136, 417–430.

Bemis, S.P., Micklethwaite, S., Turner, D., James, M.R., Akciz, S., Thiele, S.T., Bangash, H.A., 2014. Ground-based and UAV-Based photogrammetry: a multi-scale, high-resolution mapping tool for structural geology and paleoseismology. J. Struct. Geol. 69, 163–178.

Bergh, S.G., Andresen, A., 1990. Structural development of the tertiary fold-and-thrust belt in east oscar II land, spitsbergen. Polar Res. 8 (2), 217–236.

Bergh, S.G., Braathen, A., Andresen, A., 1997. Interaction of basement-involved and thin-skinned tectonism in the Tertiary fold-thrust belt of central Spitsbergen, Svalbard. AAPG (Am. Assoc. Pet. Geol.) Bull. 81 (4), 637–661.

Betlem, P., 2021. Svalbox-DOM_2020-0002_Janusfjellet.

Betlem, P., Rodés, N., 2021. Svalbox-DOM_2020-0003_Eistradalen-West.

Betlem, P., Senger, K., 2022. Svalbox-DOM_2020-0001_Festningen.

Betlem, P., Birchall, T., Ogata, K., Park, J., Skurtveit, E., Senger, K., 2020. Digital drill core models: structure-from-motion as a tool for the characterisation, orientation, and digital archiving of drill core samples. Rem. Sens. 12 (2), 21.

Betlem, P., Rodes, N., Birchall, T., Dahlin, A., Smyrak-Sikora, A., Senger, K., (in review). The Svalbox Digital Model Database: a Geoscientific Window to the High Arctic. Geosphere.

Betlem, P., Rodes, N., Horota, R., van Hazendonk, L., Svalbox Team, 2022a. Svalbox-DOM_2021-0002_Akseløya.

Betlem, P., Rodes, N., Horota, R., van Hazendonk, L., Svalbox Team, 2022b. Svalbox-DOM_2021-0009_Firkanten.

Betlem, P., Rodes, N., Horota, R., van Hazendonk, L., Svalbox Team, 2022c. Svalbox-DOM_2021-0018_Midterhuken.

Blinova, M., Thorsen, R., Mjelde, R., Faleide, J.I., 2009. Structure and evolution of the bellsund graben between forlandsundet and bellsund (spitsbergen) based on marine seismic data. Seismic study along the west Spitsbergen continental margin and adjacent area of the West Spitsbergen Fold and Thrust Belt (Isfjorden). Norw. J. Geol. 89, 215–228.

Blinova, M., Faleide, J.I., Gabrielsen, R.H., Mjelde, R., 2012. Seafloor expression and shallow structure of a fold-and-thrust system, Isfjorden, west Spitsbergen. Polar Res. 31, 13, 11209.

Blinova, M., Faleide, J.I., Gabrielsen, R.H., Mjelde, R., 2013. Analysis of structural trends of sub-sea-floor strata in the Isfjorden area of the West Spitsbergen Fold-and-Thrust Belt based on multichannel seismic data. J. Geol. Soc. 170, 657–668.

Bond, C.E., Cawood, A.J., 2021. A role for virtual outcrop models in blended learning–improved 3D thinking and positive perceptions of learning. Geoscience Communication 4 (2), 233–244.
Boyle, A., Maguire, S., Martin, A., Milsom, C., Nash, R., Rawlinson, S., Turner, A., Wurthmann, S., Conchie, S., 2007. Fieldwork is good: the student perception and the affective domain. J. Geogr. High Educ. 31 (2), 299–317.
Braathen, A., Bergh, S.G., 1995. Kinematics of Tertiary deformation in the basement-involved fold-thrust complex, western Nordenskiöld Land, Svalbard: tectonic implications based on fault-slip data analysis. Tectonophysics 249 (1), 1–29.
Braathen, A., Bergh, S., Maher, H.D., 1995. Structural outline of a Tertiary Basement-cored uplift/inversion structure in western Spitsbergen, Svalbard: kinematics and controlling factors. Tectonics 14 (1), 95–119.
Braathen, A., Bergh, S.G., Maher Jr., H.D., 1999. Application of a critical wedge taper model to the Tertiary transpressional fold-thrust belt on Spitsbergen, Svalbard. Geol. Soc. Am. Bull. 111 (10), 1468–1485.
Braathen, A., Bælum, K., Christiansen, H.H., Dahl, T., Eiken, O., Elvebakk, H., Hansen, F., Hanssen, T.H., Jochmann, M., Johansen, T.A., Johnsen, H., Larsen, L., Lie, T., Mertes, J., Mørk, A., Mørk, M.B., Nemec, W., Olaussen, S., Oye, V., Rød, K., Titlestad, G.O., Tveranger, J., Vagle, K., 2012. The Longyearbyen CO_2 Lab of Svalbard, Norway—initial assessment of the geological conditions for CO_2 sequestration. Norw. J. Geol. 353–376.
Braathen, A., Osmundsen, P.T., Maher, H., Ganerød, M., 2018. The keisarhjelmen detachment records silurian–devonian extensional collapse in northern svalbard. Terra. Nova 30 (1), 34–39.
Brugmans, P.J., 2008. Oljeleting på Svalbard; en glemt del av Norsk oljehistorie [Oil exploration on Svalbard: a forgotten part of Norway's oil history]. Store Norske Spitsbergen Kulkompani, ISBN 8299246296 (in Norwegian).
Buckley, S.J., Howell, J.A., Enge, H.D., Kurz, T.H., 2008. Terrestrial laser scanning in geology: data acquisition, processing and accuracy considerations. J. Geol. Soc. 165 (3), 625–638.
Buckley, S.J., Ringdal, K., Naumann, N., Dolva, B., Kurz, T.H., Howell, J.A., Dewez, T.J., 2019. LIME: software for 3-D visualization, interpretation, and communication of virtual geoscience models. Geosphere 15 (1), 222–235.
Buckley, S.J., Howell, J.A., Naumann, N., Lewis, C., Chmielewska, M., Ringdal, K., Vanbiervliet, J., Tong, B., Mulelid-Tynes, O.S., Foster, D., 2022. V3Geo: a cloud-based repository for virtual 3D models in geoscience. Geoscience Communication 1–27.
Carbonell Carrera, C., Bermejo Asensio, L.A., 2017. Augmented reality as a digital teaching environment to develop spatial thinking. Cartogr. Geogr. Inf. Sci. 44 (3), 259–270.
Cawood, A.J., Bond, C.E., 2019. eRock: an open-access repository of virtual outcrops for geoscience education. Geol. Soc. Am., GSA Today 29, 36–37.
Chesley, J., Leier, A., White, S., Torres, R., 2017. Using unmanned aerial vehicles and structure-from-motion photogrammetry to characterize sedimentary outcrops: an example from the Morrison Formation, Utah, USA. Sediment. Geol. 354, 1–8.
Dallmann, W., 2015. Geoscience atlas of svalbard. Norsk Polarinstitutt Rapportserie 148, 292.
Dolphin, G., Dutchak, A., Karchewski, B., Cooper, J., 2019. Virtual field experiences in introductory geology: addressing a capacity problem, but finding a pedagogical one. J. Geosci. Educ. 67 (2), 114–130.
Eiken, O., 1994. Norsk Polarinstitutt Meddelelser #130. In: Seismic Atlas of Western Svalbard : a Selection of Regional Seismic Transects. Norsk polarinstitutt, Oslo, p. 73.
Eiken, O., Degutsch, M., Riste, P., Rød, K., 1989. Snowstreamer: an efficient tool in seismic acquisition. First Break 7 (9), 374–378.
Gilley, B., Atchison, C., Feig, A., Stokes, A., 2015. Impact of inclusive field trips. Nat. Geosci. 8 (8), 579–580.
Glørstad-Clark, E., Birkeland, E.P., Nystuen, J.P., Faleide, J.I., Midtkandal, I., 2011. Triassic platform-margin deltas in the western Barents Sea. Mar. Petrol. Geol. 28 (7), 1294–1314.
Goelles, T., Hammer, T., Muckenhuber, S., Schlager, B., Abermann, J., Bauer, C., Expósito Jiménez, V.J., Schöner, W., Schratter, M., Schrei, B., 2022. MOLISENS: a modular MObile LIdar SENsor System to exploit the potential of automotive lidar for geoscientific applications. Geoscientific Instrumentation, Methods and Data Systems Discussions 1–22.
Gonzaga, J.L., Veronez, M., Kannenberg, G., Alves, D., Santana, L., Fraga, J.d., Inocencio, L., Souza, L.d., Boirdin, F., Tognoli, F., Senger, K., Cazarin, C., 2018. Mosis – multi-outcrop sharing & interpretation system. IEEE Geoscience and Remote Sensing Magazine 6 (2).
Grantz, A., Scott, R.A., Drachev, S.S., Moore, T.E., Valin, Z.C., 2011. Sedimentary successions of the Arctic Region (58–64 to 90 N) that may be prospective for hydrocarbons. Geological Society, London, Memoirs 35 (1), 17–37.
Grundvåg, S.-A., Marin, D., Kairanov, B., Śliwińska, K., Nøhr-Hansen, H., Escalona, A., Olaussen, S., 2017. The lower cretaceous succession of the northwestern Barents shelf: onshore and offshore correlations. Mar. Petrol. Geol. 86 (9), 834–857.
Harding, C., Hasiuk, F., Wood, A., 2021. TouchTerrain—3D printable terrain models. ISPRS Int. J. Geo-Inf. 10 (3), 108.
Harland, W.B., Horsfield, W.T., 1974. West Spitsbergen orogen. Geological Society, London, Special Publications 4 (1), 747–755.
Hasiuk, F., Harding, C., 2016. Touchable topography: 3D printing elevation data and structural models to overcome the issue of scale. Geol. Today 32 (1), 16–20.
Helland-Hansen, W., Grundvåg, S.-A., 2020. The svalbard eocene-oligocene (?) central basin succession: sedimentation patterns and controls. Basin Res. 33 (1), 729–753.
Henriksen, E., Ryseth, A.E., Larssen, G.B., Heide, T., Rønning, K., Sollid, K., Stoupakova, A.V., 2011. Chapter 10 Tectonostratigraphy of the greater Barents Sea: implications for petroleum systems. In: Spencer, A.M., Embry, A.F., Gautier, D.L., Stoupakova, A.V., Sørensen, K. (Eds.), Arctic Petroleum Geology. The Geological Society, London, pp. 163–195.
Hodgetts, D., 2013. Laser scanning and digital outcrop geology in the petroleum industry: a review. Mar. Petrol. Geol. 46, 335–354.
Horota, R.K., 2021. AG-210 VFT: Aldegondabreen. Roundme.com. Retrieved January 7, 2023. https://Roundme.com. https://roundme.com/tour/756817/view/2386203/.
Horota, R.K., 2022. The Paleogene transpression. VRSVALBARD.COM. Retrieved January 7, 2023. https://vrsvalbard.com/the-paleogene-transpression.
Horota, R.K., Rossa, P., Marques, A., Gonzaga, L., Senger, K., Cazarin, C.L., et al., 2022a. An Immersive Virtual Field Experience Structuring Method for Geoscience Education. In: IEEE Transactions on Learning Technologies.
Horota, R.K., Senger, K., Rodes, N., Betlem, P., Smyrak-Sikora, A., Jonassen, M.O., Kramer, D., Braathen, A., 2022b. West Spitsbergen Fold and Thrust Belt: a Digital Educational Data Package for Teaching Structural Geology.
Howell, J.A., Martinius, A.W., Good, T.R., 2014. The application of outcrop analogues in geological modelling: a review, present status and future outlook. In: Martinius, A. W., Howell, J.A., Good, T.R. (Eds.), Sediment-Body Geometry and Heterogeneity: Analogue Studies for Modelling the Subsurface. Geological Society of London, London, pp. 1–25.
Janocha, J., Smyrak-Sikora, A., Senger, K., Birchall, T., 2020. Seeing beyond the outcrop: integration of ground-penetrating radar with digital outcrop models of a paleokarst system. Mar. Petrol. Geol., 104833
Janocha, J., Lord, G., Rodes, N., Betlem, P., 2021. Svalbox-DOM_2020-0007_ Varmlandsryggen.
Johannessen, E.P., Henningsen, T., Bakke, N.E., Johansen, T.A., Ruud, B.O., Riste, P., Elvebakk, H., Jochmann, M., Elvebakk, G., Woldengen, M.S., 2011. Palaeogene clinoform succession on Svalbard expressed in outcrops, seismic data, logs and cores. First Break 29, 35–44.
Johansen, S.E., Andresen, A., Kibsgaard, S., Henningsen, T., Granli, J.R., 1994. Seismic modeling of a strongly emergent thrust front, West Spitsbergen fold belt, svalbard. Journal name: AAPG bulletin (American association of petroleum geologists); (United States). Journal 78 (7), 1018–1027. Medium: X; Size.
Johansen, T.A., Ruud, B.O., Bakke, N.E., Riste, P., Johannessen, E.P., Henningsen, T., 2011. Seismic profiling on Arctic glaciers. First Break 29, 7.
Kartverket, Steatens, 2022. Bathymetric Data for Norway.
Kastens, K.A., Ishikawa, T., 2006. Spatial thinking in the geosciences and cognitive sciences: a cross-disciplinary look at the intersection of the two fields. Spec. Pap. Geol. Soc. Am. 413, 53.
Kastens, K.A., Manduca, C.A., Cervato, C., Frodeman, R., Goodwin, C., Liben, L.S., Mogk, D.W., Spangler, T.C., Stillings, N.A., Titus, S., 2009. How geoscientists think and learn. Eos, Transactions American Geophysical Union 90 (31), 265–266.
Klausen, T.G., Nyberg, B., Helland-Hansen, W., 2019. The largest delta plain in Earth's history. Geology 47 (5), 470–474.
Koevoets, M.J., Hammer, Ø., Olaussen, S., Senger, K., Smelror, M., 2018. Integrating subsurface and outcrop data of the middle jurassic to lower cretaceous agardfjellet formation in central spitsbergen. Norw. J. Geol. 98 (1), 1–34.
Laporte, K., 2022. Exploring the Potential of an Interactive Geoscience Teaching Application for Dynamically Visualizing 3D Terrain in Undergraduate Classrooms.
Larsen, T., 2009. Fractured Carbonates in the Mediumfjellet Thrust-Stack in the Tertiary Fold-And-Thrust Belt of Spitsbergen, Universitetet I Tromsø.
Lasabuda, A.P.E., Johansen, N.J.S., Laberg, J.S., Faleide, J.I., Senger, K., Rydningen, T. A., Patton, H., Knutsen, S.-M., Hanssen, A., 2021. Cenozoic uplift and erosion of the Norwegian Barents Shelf – a review. Earth Sci. Rev. 217, 1–35.
Leever, K.A., Gabrielsen, R.H., Faleide, J.I., Braathen, A., 2011. A transpressional origin for the West Spitsbergen fold-and-thrust belt: insight from analog modeling. Tectonics 30 (2, TC2014), 1–24.
Lord, G., Janocha, J., Rodes, N., Betlem, P., 2021. Svalbox-DOM_2020-0015_ Lagmannstoppen-East.
Luetzenburg, G., Kroon, A., Bjørk, A.A., 2021. Evaluation of the apple iPhone 12 pro LiDAR for an application in geosciences. Sci. Rep. 11 (1), 1–9.
Lundmark, A.M., Augland, L.E., Jørgensen, S.V., 2020. Digital fieldwork with Fieldmove - how do digital tools influence geoscience students' learning experience in the field? J. Geogr. High Educ. 1–14.
Lundschien, B.A., Høy, T., Mørk, A., 2014. Triassic hydrocarbon potential in the Northern Barents Sea; integrating Svalbard and stratigraphic core data. Norwegian Petroleum Directorate Bulletin 11, 3–20.
Maher Jr., H.D., Craddock, C., Maher, K., 1986. Kinematics of tertiary structures in upper paleozoic and mesozoic strata on midterhuken, West Spitsbergen. Geol. Soc. Am. Bull. 97 (12), 1411–1421.
Maher Jr., H.D., Braathen, A., Bergh, S., Dallmann, W., Harland, W.B., 1995. Tertiary or Cretaceous age for Spitsbergen's fold-thrust belt on the Barents Shelf. Tectonics 14 (6), 1321–1326.
Maher, H., Braathen, A., Ganerød, M., Osmundsen, P.T., Redfield, t., Myhre, P.I., Serck, C., Parcher, S., 2022. Core complex fault rocks of the silurian to devonian keisarhjelmen detachment in NW spitsbergen. In: Kuiper, Y.D., Murphy, J.B., Nance, R.D., Strachan, R.A., Thompson, M.D. (Eds.), New Developments in the Appalachian-Caledonian-Variscan Orogen.
Marques Jr., A., Horota, R.K., de Souza, E.M., Lupssinskü, L., Rossa, P., Aires, A.S., Bachi, L., Veronez, M.R., Gonzaga Jr., L., Cazarin, C.L., 2020. Virtual and digital outcrops in the petroleum industry: a systematic review. Earth Sci. Rev., 103260
Midtkandal, I., Nystuen, J.P., 2009. Depositional architecture of a low-gradient ramp shelf in an epicontinental sea: the lower Cretaceous of Svalbard. Basin Res. 21 (5), 655–675.
Midtkandal, I., Faleide, J.I., Faleide, T.S., Serck, C.S., Planke, S., Corseri, R., Dimitriou, M., Nystuen, J.P., 2019. Lower Cretaceous Barents Sea strata:

epicontinental basin configuration, timing, correlation and depositional dynamics. Geol. Mag. 1–19.
Minakov, A., 2018. Late Cenozoic lithosphere dynamics in Svalbard: interplay of glaciation, seafloor spreading and mantle convection. J. Geodyn. 122, 1–16.
Mulrooney, M.J., Larsen, L., Stappen, J.V., Cnudde, V., Senger, K., Rismyhr, B., Braathen, A., Olaussen, S., Mørk, M.B.E., Ogata, K., 2019. Fluid flow properties of the Wilhelmøya Subgroup, a potential unconventional CO_2 storage unit in central Spitsbergen. Norw. J. Geol. 99, 85–116.
Nesbit, P.R., Boulding, A.D., Hugenholtz, C.H., Durkin, P.R., Hubbard, S.M., 2020. Visualization and sharing of 3D digital outcrop models to promote open science. GSA Today (Geol. Soc. Am.) 30 (6).
Norwegian Polar Institute, 2014a. Geological and Topographic Data from Svalbard: Geodata (npolar.no).
Norwegian Polar Institute, 2014b. Terrengmodell Svalbard (S0 Terrengmodell).
Norwegian Polar Institute, 2016. Geological map of Svalbard 1, 250000.
Norwegian Polar Institute, 2022a. Basemap Services.
Norwegian Polar Institute, 2022b. NP_Basiskart_Svalbard_WMTS_25833.
Ogata, K., Senger, K., Braathen, A., Tveranger, J., Olaussen, S., 2014. Fracture systems and meso-scale structural patterns in the siliciclastic Mesozoic reservoir-caprock succession of the Longyearbyen CO2 Lab project: implications for geologic CO2 sequestration on Central Spitsbergen, Svalbard. Norw. J. Geol. 94, 121–154.
Olaussen, S., Senger, K., Braathen, A., Grundvåg, S.A., Mørk, A., 2019. You learn as long as you drill; research synthesis from the Longyearbyen CO2 Laboratory, Svalbard, Norway. Norw. J. Geol. 99, 157–187.
Olaussen, S., Grundvåg, S.-A., Senger, K., Anell, I., Betlem, P., Birchall, T., Braathen, A., Dallmann, W., Johannessen, E.P., Lord, G., Mørk, A., Osmundsen, P.T., Smyrak-Sikora, A., Stemmerik, L., 2023. Svalbard Composite Tectono-Stratigraphic Element. High Arctic Norway Geological Society of London Memoirs. M., J.
Piepjohn, K., 2000. The svalbardian-ellesmerian deformation of the Old red sandstone and the pre-devonian basement in NW spitsbergen (svalbard). Geological Society, London, Special Publications 180 (1), 585–601.
Pringle, J.K., Howell, J.A., Hodgetts, D., Westerman, A.R., Hodgson, D.M., 2006. Virtual outcrop models of petroleum reservoir analogues: a review of the current state-of-the-art. First Break 24, 33–42.
Pugsley, J.H., Howell, J.A., Hartley, A., Buckley, S.J., Brackenridge, R., Schofield, N., Maxwell, G., Chmielewska, M., Ringdal, K., Naumann, N., 2021. Virtual Fieldtrips: construction, delivery, and implications for future geological fieldtrips. Geoscience Communication Discussions 1–33.
Rarity, F., Van Lanen, X., Hodgetts, D., Gawthorpe, R., Wilson, P., Fabuel-Perez, I., Redfern, J., 2014. LiDAR-based digital outcrops for sedimentological analysis: workflows and techniques. Geological Society, London, Special Publications 387 (1), 153–183.
Rittersbacher, A., Buckley, S.J., Howell, J.A., Hampson, G.J., Vallet, J., 2013. Helicopter-based laser scanning: a method for quantitative analysis of large-scale sedimentary architecture. In: Martinius, A.W., Howell, J.A., Good, T. (Eds.), Sediment-body Geometry and Heterogeneity: Analogue Studies for Modelling the Subsurface. Geological Society of London Special Publication #387, London, pp. 1–18.
Roach, M., 2019. AusGeol – the virtual library of Australia's geology. In: Kampmann, T. C. (Ed.), Visual3D Conference 2019, pp. 1–2. Uppsala, Sweden, October 2019.
Roy, S., Hovland, M., Noormets, R., Olaussen, S., 2015. Seepage in isfjorden and its tributary fjords, West Spitsbergen. Mar. Geol. 363, 146–159.
Roy, S., Senger, K., Hovland, M., Römer, M., Braathen, A., 2019. Geological controls on shallow gas distribution and seafloor seepage in Arctic fjord of Spitsbergen, Norway. Mar. Petrol. Geol. 107 (9), 237–254.
Senger, K., Galland, O., 2022. Stratigraphic and spatial extent of HALIP magmatism in central spitsbergen. G-cubed, e2021GC010300.
Senger, K., Nordmo, I., 2021. Using digital field notebooks in geoscientific learning in polar environments. J. Geosci. Educ. 69 (2), 166–177.
Senger, K., Roy, S., Braathen, A., Buckley, S.J., Bælum, K., Gernigon, L., Mjelde, R., Noormets, R., Ogata, K., Olaussen, S., Planke, S., Ruud, B.O., Tveranger, J., 2013. Geometries of doleritic intrusions in central Spitsbergen, Svalbard: an integrated study of an onshore-offshore magmatic province with implications on CO_2 sequestration. Norw. J. Geol. 93, 143–166.
Senger, K., Planke, S., Polteau, S., Svensen, H., Ogata, K., 2014a. Sill emplacement and contact metamorphism in a siliciclastic reservoir on Svalbard, Arctic Norway. Norw. J. Geol. 94 (2–3), 155–169.
Senger, K., Tveranger, J., Ogata, K., Braathen, A., Planke, S., 2014b. Late mesozoic magmatism in svalbard: a review. Earth Sci. Rev. 139, 123–144.
Senger, K., Brugmans, P., Grundvåg, S.-A., Jochmann, M., Nøttvedt, A., Olaussen, S., Skotte, A., Smyrak-Sikora, A., 2019. Petroleum exploration and research drilling onshore Svalbard: a historical perspective. Norw. J. Geol. 99 (3), 1–30.
Senger, K., Betlem, P., Birchall, T., Buckley, S.J., Coakley, B., Eide, C.H., Flaig, P.P., Forien, M., Galland, O., Gonzaga Jr., L., Jensen, M., Kurz, T., Lecomte, I., Mair, K., Malm, R., Mulrooney, M., Naumann, N., Nordmo, I., Nolde, N., Ogata, K., Rabbel, O., Schaaf, N.W., Smyrak-Sikora, A., 2021a. Using digital outcrops to make the high Arctic more accessible through the Svalbox database. J. Geosci. Educ. 69, 123–137.
Senger, K., Betlem, P., Grundvåg, S.-A., Horota, R.K., Buckley, S.J., Smyrak-Sikora, A., Jochmann, M.M., Birchall, T., Janocha, J., Ogata, K., 2021b. Teaching with digital geology in the high Arctic: opportunities and challenges. Geoscience Communication 4 (3), 399–420.
Senger, K., Betlem, P., Grundvåg, S.-A., Horota, R.K., Buckley, S.J., Smyrak-Sikora, A., Jochmann, M.M., Birchall, T., Janocha, J., Ogata, K., Kuckero, L., Johannessen, R.M., Lecomte, I., Cohen, S.M., Olaussen, S., 2021c. Teaching with digital geology in the high Arctic: opportunities and challenges. Geoscience Communication 1–39.
Senger, K., Janocha, J., Rodes, N., Team", S., 2021d. Svalbox-DOM_2019-0004_Productustoppen.
Senger, K., Betlem, P., Birchall, T., Gonzaga Jr., L., Grundvåg, S.-A., Horota, R.K., Laake, A., Kuckero, L., Mørk, A., Planke, S., Rodes, N., Smyrak-Sikora, A., 2022a. Digitising Svalbard's geology: the festningen digital outcrop model. First Break 40 (3), 47–55.
Senger, K., Betlem, P., Birchall Jr., T., Grundvåg, S.-A., Horota, R.K., Laake, A., Kuckero, L., Mørk, A., Planke, S., Rodes, N., Smyrak-Sikora, A., 2022b. Digitizing Svalbard's Geology: the Festningen Digital Outcrop Model. First Break. L.G.
Smyrak-Sikora, A., Nicolaisen, J., Braathen, A., Johannessen, E.P., Olaussen, S., Stemmerik, L., 2021. Impact of growth faults on mixed siliciclastic-carbonate-evaporite deposits during rift climax and reorganisation—Billefjorden Trough, Svalbard, Norway. Basin Res. 1–32.
Sorento, T., Olaussen, S., Stemmerik, L., 2020. Controls on deposition of shallow marine carbonates and evaporites–lower Permian Gipshuken Formation, central Spitsbergen, Arctic Norway. Sedimentology 67 (1), 207–238.
Steel, R.J., Worsley, D., 1984. Svalbard's post-Caledonian strata - an atlas of sedimentational patterns and paleogeographic evolution. In: Spencer, A.M. (Ed.), Petroleum Geology of the North European Margin. Graham & Trotman, London, pp. 109–135.
Stemmerik, L., Worsley, D., 2005. 30 years on – Arctic Upper Palaeozoic stratigraphy, depositional evolution and hydrocarbon prospectivity. Norw. J. Geol. 85, 151–168.
Tavani, S., Billi, A., Corradetti, A., Mercuri, M., Bosman, A., Cuffaro, M., Seers, T., Carminati, E., 2022. Smartphone assisted fieldwork: towards the digital transition of geoscience fieldwork using LiDAR-equipped iPhones. Earth Sci. Rev., 103969
Vollgger, S.A., Cruden, A.R., 2016. Mapping folds and fractures in basement and cover rocks using UAV photogrammetry, Cape Liptrap and Cape Paterson, Victoria, Australia. J. Struct. Geol. 85, 168–187.
Welbon, A.I., Maher, H.D., 1992. Tertiary tectonism and basin inversion of the St. Jonsfjorden region, Svalbard. J. Struct. Geol. 14 (1), 41–55.
Wesenlund, F., Grundvåg, S.-A., Engelschiøn, V.S., Thießen, O., Pedersen, J.H., 2021. Linking facies variations, organic carbon richness and bulk bitumen content–A case study of the organic-rich Middle Triassic shales from eastern Svalbard. Mar. Petrol. Geol. 132, 105168.
Westoby, M., Brasington, J., Glasser, N., Hambrey, M., Reynolds, J., 2012. 'Structure-from-Motion'photogrammetry: a low-cost, effective tool for geoscience applications. Geomorphology 179, 300–314.
Worsley, D., 2008. The post-Caledonian development of Svalbard and the western Barents Sea. Polar Res. 27, 298–317.